

Is Lattice Quantum Gravity Asymptotically Safe ?

Making contact between Causal Dynamical Triangulations and the Functional Renormalization Group.

J. Ambjørn,^{1, 2, *} J. Gizbert-Studnicki,^{3, 4, †} A. Görlich,^{3, 4, ‡} and D. Németh^{2, §}

¹*The Niels Bohr Institute, Copenhagen University Blegdamsvej 17, DK-2100 Copenhagen Ø, Denmark.*

²*Institute for Mathematics, Astrophysics and Particle Physics (IMAPP) Radboud University Nijmegen,
Heyendaalseweg 135, 6525 AJ Nijmegen, The Netherlands*

³*Institute of Theoretical Physics, Jagiellonian University,*

ul. prof. S. Łojasiewicza 11, Kraków, PL 30-348, Poland.

⁴*Mark Kac Center for Complex Systems Research, Jagiellonian University,
ul. prof. S. Łojasiewicza 11, Kraków, PL 30-348, Poland.*

We compare the effective action of the scale factor obtained from lattice quantum gravity (in the form of Causal Dynamical Triangulations (CDT)) to the corresponding effective action obtained from the simplest Functional Renormalization Group (FRG) calculation. In this way, we can identify the generic infinite four-volume limit of the lattice theory in the so-called de Sitter phase with the Gaussian fixed-point limit or the IR fixed-point limit obtained by FRG. We also show how to identify a putative UV lattice gravity fixed point. Our Monte Carlo simulations of CDT allow for the existence of such a UV fixed point, although the data precision does not yet provide a proof of its existence. The concept of a correlation length relevant for the lattice gravity fixed points is argued to be different from the concept of correlation lengths encountered in field theories in a fixed spacetime background.

* ambjorn@nbi.dk, ambjorn@science.ru.nl

† jakub.gizbert-studnicki@uj.edu.pl

‡ andrzej.goerlich@uj.edu.pl

§ nemeth.daniel.1992@gmail.com

I. INTRODUCTION

Four-dimensional Causal Dynamical Triangulations (CDT) attempts to provide a lattice regularization of four-dimensional quantum gravity (see [1, 2] for reviews). The path integral is defined as a sum over a certain class of piecewise linear geometries and the length a of the links of the triangulations defining the piecewise linear geometries acts as a UV cut-off, precisely as for ordinary lattice field theories. The main difference between ordinary lattice field theories and CDT is that the lattice in the former case is fixed, the dynamics coming from the fields that “live” on the lattice, while for CDT the dynamics originates from summing over different lattices, representing different geometries in the path integral.

The CDT program assumes that there exists a continuum 4d quantum field theory of gravity, and the task is then to study the lattice theory and show that one can fine tune the dimensionless bare coupling constants of the lattice theory in such a way that one can take the lattice cut-off $a \rightarrow 0$ and still obtain an interacting quantum theory. This is a non-trivial task even for a standard renormalizable quantum field theory, and here it becomes even more difficult since quantum gravity is not a perturbatively renormalizable quantum field theory in four dimensions. The possibility that there might exist such a non-perturbatively renormalizable theory of gravity is known as the asymptotic safety scenario [3]. A lot of work has gone into testing this scenario using what is known as the Functional Renormalization Group approach (FRG), and there is good evidence that such a scenario could be true (see [4–6] for extensive reviews). However, even if there exists a non-perturbative UV fixed point where one can define a theory of quantum gravity, it is not clear that the corresponding theory will be a unitary theory. The unitarity problem is even older than the asymptotic safety scenario, since one can add R^2 terms to the Einstein-Hilbert action and then the theory can be formulated as a renormalizable theory [7], but the problem is that it will in general be a non-unitary theory and this is one reason it was originally not considered as a viable quantum gravity candidate.

When solving the FRG equations in order to locate the non-perturbative UV fixed point one has to truncate the equations and it is difficult to judge how reliable such truncations are. It is therefore very desirable to verify the existence of the UV fixed point by an independent approach, and lattice gravity in the form of CDT is such an approach. It is based on Monte Carlo simulations and thus it will also involve approximations, but of a quite different nature than those used in the FRG equations. Also, it should be mentioned that the lattice CDT theory is a unitary theory¹. Thus, if the lattice results can confirm the FRG picture, it provides evidence in favor of the non-perturbative theory defined at the (putative) UV fixed point being a unitary theory. Also, for the same reason it is unlikely that the continuum limit of the lattice theory, should it be non-trivial, can be viewed as a continuum quantum gravity theory with a simple R^2 term added to the Einstein-Hilbert terms.

The lattice action used in the CDT lattice theory depends on three dimensionless coupling constants. In this coupling constant space there are critical surfaces, defining phase transitions of the lattice theory. These critical surfaces intersect at critical lines and a UV fixed point could be positioned on such critical lines. The purpose of this article is to report on Monte Carlo measurements close to some of the critical lines and to compare the effective action obtained from the Monte Carlo simulations with the effective action obtained by continuum FRG calculations.

II. FRG

The very simplest effective action obtained by the FRG is a truncation where one considers the Einstein-Hilbert action with the gravitational coupling constant G and the cosmological constant Λ as functions of the so-called scale k entering the FRG equations. The corresponding effective action in spacetimes with Euclidean signature can then be written as

$$\Gamma_k[g_{\mu\nu}] = \frac{1}{16\pi G_k} \int d^4x \sqrt{g(x)} \left(-R(x) + 2\Lambda_k \right) \quad (1)$$

The running coupling constants are conjectured to have an UV fixed point for $k \rightarrow \infty$, where they behave as

$$G_k := g_k/k^2, \quad g_k \rightarrow g_*, \quad \Lambda_k := \lambda_k k^2, \quad \lambda_k \rightarrow \lambda_*, \quad (2)$$

where g_k and λ_k are dimensionless coupling constants that one might try to compare to suitable dimensionless lattice gravity coupling constants. In particular we have for the dimensionless combination $G_k \Lambda_k$:

$$G_k \Lambda_k \rightarrow g_* \lambda_* \quad \text{for } k \rightarrow \infty. \quad (3)$$

¹ More precisely, after rotating to Euclidean signature in CDT, one can define a transfer matrix with respect to the CDT Euclidean time and show that it is reflection positive [8]. In lattice field theories this ensures that one will obtain a unitary time evolution when rotating back to the Lorentzian signature.

Let us treat (1) as a standard effective action². Then an extremum for $\Gamma_k[g_{\mu\nu}]$ is a de Sitter universe with cosmological constant Λ_k . We will assume the metric is Euclidean and then the solution is a four-sphere, S^4 , with radius $R_k = 3/\sqrt{\Lambda_k}$. One can now study fluctuations around this solution. We will only do that here in the simplest possible way where we use a minisuperspace version of (1). The reason for this restriction is that we want to compare with computer simulations of quantum gravity, in the version of CDT, where such a minisuperspace effective action appears when one integrates (numerically, via Monte Carlo simulations) over all degrees of freedom except the scale factor $r(t)$ or the three-volume $V_3(t)$ defined in eqs. (5) and (7)³. Close to the UV fixed point we then have

$$R_k = \frac{3}{\sqrt{\lambda_k}} \frac{1}{k} \rightarrow \frac{3}{\sqrt{\lambda_*}} \frac{1}{k}, \quad V_4(k) = \frac{8\pi^2}{3} R_k^4 = \frac{8\pi^2}{3} \frac{81}{\lambda_k^2} \frac{1}{k^4} \rightarrow \frac{8\pi^2}{3} \frac{81}{\lambda_*^2} \frac{1}{k^4}, \quad (4)$$

i.e. the volume $V_4(k)$ of the de Sitter sphere goes to zero when approaching the UV fixed point. Does it make sense to study fluctuations “around” such small universe? Somewhat surprisingly the answer is affirmative because the coupling constant appearing in the study of fluctuations is $\sqrt{G_k \Lambda_k} = \sqrt{g_k \lambda_k}$ that is never large, even at the UV fixed point where R_k formally is zero. In order to compare with computer simulations let us consider fluctuations around a de Sitter sphere with fixed volume V_4 rather than fixed Λ . The minisuperspace action written using the metric

$$ds^2 = dt^2 + r^2(t) d\Omega_3^2, \quad (5)$$

where t denotes a choice of proper time and $d\Omega_3^2$ the squared line element on the unit three-sphere, is

$$S = -\frac{1}{24\pi G_k} \int dt \left(\frac{\dot{V}_3^2}{V_3} + \delta_0 V_3^{1/3} \right), \quad \int dt V_3(t) = V_4(k), \quad (6)$$

where

$$V_3(t) = 2\pi^2 r^3(t), \quad \delta_0 = 9(2\pi^2)^{2/3}. \quad (7)$$

Introducing dimensionless variables $v_3 = V_3/V_4^{3/4}$ and $s = t/V_4^{1/4}$ we can write

$$S = -\frac{1}{24\pi} \frac{\sqrt{V_4(k)}}{G_k} \int ds \left(\frac{\dot{v}_3^2}{v_3} + \delta_0 v_3^{1/3} \right), \quad \int ds v_3(s) = 1. \quad (8)$$

Here s and $v_3(s)$ will be of order $O(1)$ and the classical solution (the four-sphere with volume 1) is

$$v_3^{cl}(s) = \frac{3}{4\omega_0} \cos^3 \left(\frac{s}{\omega_0} \right), \quad \omega_0^4 = \frac{3^4}{2^2} \frac{1}{\delta_0^{3/2}} = \frac{3}{8\pi^2}, \quad s \in \left[-\frac{\pi\omega_0}{2}, \frac{\pi\omega_0}{2} \right]. \quad (9)$$

The fluctuations around $v_3^{cl}(s)$ will for a given k be governed by the effective coupling constant

$$g_{\text{eff}}^2(k) = \frac{24\pi G_k}{\sqrt{V_4(k)}} = \frac{4}{\sqrt{6}} \Lambda_k G_k \simeq 1.63 \lambda_k g_k. \quad (10)$$

In the FRG analysis $\lambda_k g_k$ will be running from the present days value for small $k = k_p$ ($\lambda_{k_p} g_{k_p} \approx 10^{-120}$) to the value $\lambda_* g_*$. This UV fixed point value is not really universal, but with a number of different regularizations one finds values like $\lambda_* g_* = 0.12 \pm 0.02$ (see [4], Table 2); on the other hand, a recent calculation, including wave function renormalization in the calculation and using a different regularization, finds $\lambda_* g_* = 0.74 10^{-3}$ [12], i.e. a value quite a lot lower⁴. In both cases there is no obvious obstruction to use lowest order perturbative expansion around v_3^{cl} . Denoting the fluctuations around $v_3^{cl}(s)$ by $x(s)$ we have (see [14] and [1] for details)

$$v_3(s) = v_3^{cl}(s) + x(s), \quad \frac{x(s)}{v_3^{cl}(s)} = O(g_{\text{eff}}(k)). \quad (11)$$

If we choose the two values of $\lambda_* g_*$ mentioned above we obtain

$$\frac{x(0)}{v_3^{cl}(0)} = O(g_{\text{eff}}(k)) \quad \text{where} \quad g_{\text{eff}}(k) < 0.44 \text{ or } 0.035 \quad (12)$$

for all values of k , starting at the present day small value k_p , to $k \rightarrow \infty$ when approaching the UV fixed point. It is remarkable that such a “semiclassical” description seems to be valid all the way to the UV fixed point.

² In the actual FRG calculations one is often making the decomposition $g_{\mu\nu} = g_{\mu\nu}^B + h_{\mu\nu}$, where $g_{\mu\nu}^B$ is a fixed background metric (e.g. a fixed de Sitter metric) that is fixed even when the scale k is changing. From first principles the effective action can only depend in $g_{\mu\nu}$, not the arbitrary choice $g_{\mu\nu}^B$. Our treatment here is the most naive implementation of what is suggested in [9, 10], namely that the background one should use for a given scale k should be the one that satisfy the equations of motion at that scale. In [10] it is called the choice of self-consistent background geometries.

³ In [11] it is shown that when calculating fluctuations for “global” quantities like the three-volume, only constant modes contribute when space is compact. These modes are precisely the modes used when calculating fluctuations in the minisuperspace approximation.

⁴ An earlier calculation [13], essentially using the same framework as in [12], but more general, obtained more or less agreement with the old FRG calculations, using the “standard” FRG regularization.

III. THE CDT MONTE CARLO SIMULATIONS

The piecewise linear geometries (the lattice geometries) we will consider below are constructed from building blocks (four-simplices) glued together in various ways. The length of the links, a act as a UV cut off in the same way as for ordinary lattice field theories. Before starting a detailed discussion of the class of geometries we consider, let us just assume we manage to create geometries on the computer that are representatives of the geometries close to the FRG UV fixed point. Let us further assume that close to the fixed point we loosely can identify $a \propto 1/k$. A piecewise linear lattice geometry will then be constructed from N_4 four-simplices, and each of these will have a four-volume $\sqrt{5}/96 \cdot a^4$, i.e. a total four-volume of $V_4 = \sqrt{5}/96 \cdot N_4 a^4$. We can now compare this to the FRG expression (4) for $V_4(k)$ and we obtain

$$N_4 \propto \frac{96}{\sqrt{5}} \frac{8\pi^2}{3} \frac{81}{\lambda_*^2} \quad (\approx 2 \cdot 10^6). \quad (13)$$

The approximate value is obtained by using a typical value for λ_* obtained in the FRG studies. The important point before starting the detailed discussion below is that if we write $a \propto 1/k$ close to the UV fixed point, we are led to a finite N_4 at the fixed point and we need non-trivial scaling in the lattice theory to avoid this conclusion. Below, more elaborate arguments lead to the same conclusion even if we do not assume $a \propto 1/k$ near the UV fixed point. The geometries one observes in the computer simulations depend on the choice of the bare coupling constants used in the lattice action. We denote these κ_0 , Δ , and κ_4 . We refer to [1] for a detailed discussion of the origin and interpretation of these, here we only remark that κ_0 is related to the inverse bare dimensionless gravitational coupling constant, i.e. we have

$$\kappa_0 \propto \frac{a^2}{G}, \quad (14)$$

where G denotes the gravitation coupling constant that appears in the Einstein-Hilbert action, while κ_4 is related to the dimensionless cosmological coupling constant $a^4 \Lambda/G$. Finally Δ can be related to a possible asymmetry between space and time inherent in the CDT lattice implementation of spacetime. For given values κ_0 and Δ , the coupling constant κ_4 controls the number of four-simplices, N_4 , of the lattice configuration. In a given Monte Carlo (MC) simulation it is convenient to keep N_4 (approximately) fixed. Thus κ_4 will not play a direct role as a coupling constant. However, we will perform the MC simulations for various choices of N_4 , and are interested in the limit $N_4 \rightarrow \infty$. For a given choice of κ_0 and Δ there is a critical value $\kappa_4^c(\kappa_0, \Delta)$ of κ_4 , such that for $\kappa_4 \rightarrow \kappa_4^c(\kappa_0, \Delta)$ the expectation value of $N_4 \rightarrow \infty$ if we leave N_4 unconstrained in the MC simulations. In this way we are replacing the change in coupling constant κ_4 with the change in N_4 . In the κ_0, Δ coupling constant plane there are phase transition lines⁵. These lines are boundaries for various regions in the bare coupling constant space, regions where typical geometries of the four-dimensional spacetime are very different. The phase diagram of the four-dimensional CDT model is shown in Fig. 1 and we are here interested in the region named the “de Sitter phase” or the C_{ds} phase.

We will not discuss in any detail how to implement the numerical setup (again we refer to [1]), only mention that no background geometry is enforced in the computer simulations, but a time slicing, loosely corresponding to the proper time, and that the spatial *topology* of S^3 is also imposed on the lattice configurations for each leaf of the foliation. It should be emphasized that it does not mean that the computer S^3 configurations have the nice geometry of a round S^3 sphere embedded in \mathbb{R}^4 : all possible (lattice) S^3 geometries accessible by the MC simulations. Thus the set up is as follows: each lattice geometry is defined by N_4 identical four-simplices where all links have length a and at each time slice t the three-spheres are constructed from $N_3(t)$ three-simplices (tetrahedra), also with link length a . Each such tetrahedron is shared by two four-simplices⁶. The geometry is defined uniquely by the way the four-simplices are glued together. The Monte Carlo simulations change this gluing so that, in principle, one “integrates” over all geometries which can be constructed from these building blocks, preserving the topology and the foliation. For a fixed N_4 we can now measure $\langle N_3(t) \rangle$ and $\langle N_3(t_1)N_3(t_2) \rangle$ and thus observe some simple properties of our quantum universe, as well as construct an effective action that reproduces the “observed” results. In analogy with the continuum notation above, we introduce

$$s_i = \frac{t_i}{N_4^{1/4}}, \quad n_3(s_i) = \frac{N_3(t_i)}{N_4^{3/4}}, \quad \Delta s = \frac{1}{N_4^{1/4}}, \quad (15)$$

⁵ Strictly speaking we only have genuine phase transitions in the limit $N_4 \rightarrow \infty$. However, for finite but large N_4 , one observes a “pseudo transition” where order parameters change fast. By studying the location of these changes in the κ_0, Δ plane for a number of N_4 ’s, one obtains approximate locations of the phase transitions, which can be extrapolated to $N_4 \rightarrow \infty$. Such finite-size scaling studies will allow us to find the critical exponents related to the phase transitions, as we will discuss in detail below.

⁶ These four-simplices are denoted (1, 4)-four-simplices because they have 4 vertices at the given time-slice and one vertex at the neighboring time-slice. To fill out the four-dimensional slab between two spatial time slices, one also needs the so-called (2, 3)-four-simplices, where two and three vertices are placed on the neighboring time slices. We refer to [1] for a detailed discussion.

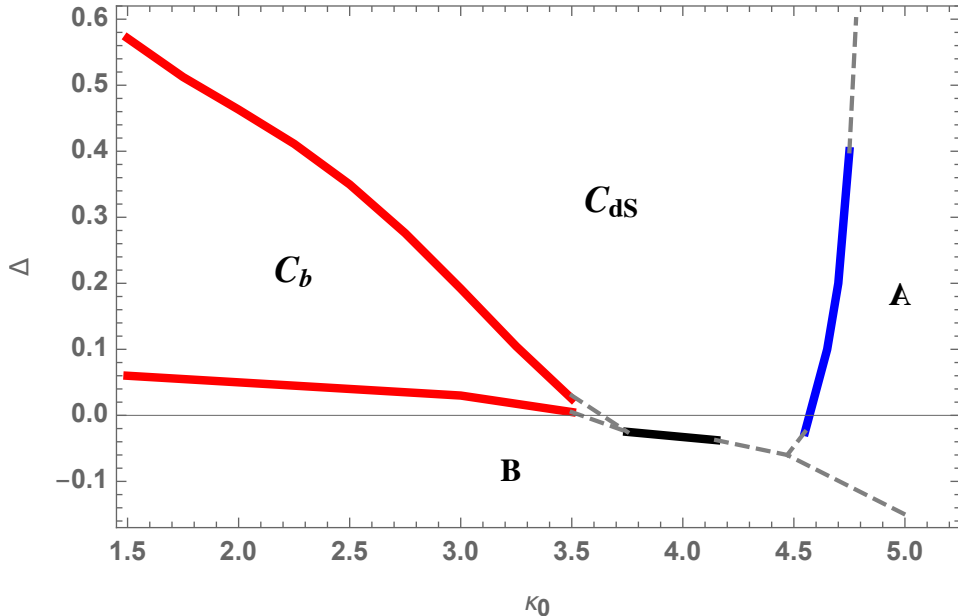


FIG. 1. The CDT phase diagram. Phase transition between phases C_{dS} and C_b is (most likely) second order, as is the transition between C_b and B , while the transition between C_{dS} and A is first order. The transition between C_{dS} and B is still under investigation.

and for given values of the bare coupling constants in the de Sitter phase we now have with high precision:

$$\langle n_3(s) \rangle = \frac{3}{4\omega} \cos^3 \left(\frac{s}{\omega} \right), \quad \frac{\delta}{\delta_0} = \left(\frac{\omega_0}{\omega} \right)^{8/3}, \quad (16)$$

$$S_{\text{eff}} = \frac{\sqrt{N_4}}{\Gamma} \int_{-\pi\omega/2}^{\pi\omega/2} ds \left(\frac{\dot{n}_3^2(s)}{n_3(s)} + \delta n_3^{1/3}(s) \right), \quad \int_{-\pi\omega/2}^{\pi\omega/2} ds n_3(s) = 1, \quad (17)$$

where S_{eff} in (17) is the large N_4 limit of

$$S_{\text{eff}} = \frac{1}{\Gamma} \sum_i \left(\frac{(N_3(t_{i+1}) - N_3(t_i))^2}{N_3(t_i)} + \delta N_3^{1/3}(t_i) \right). \quad (18)$$

We can clearly identify $\langle n_3(s) \rangle$ with the “classical” solution $n_3^{cl}(s)$ corresponding to the action (17). $n_3^{cl}(s)$ will describe an “elongated” sphere if $\delta > \delta_0$, i.e. $\omega < \omega_0$ (the radius of the spatial three-spheres $n_3^{cl}(s)$ is multiplied by a factor $(\omega_0/\omega)^{4/3}$ compared to the three-spheres that enter the description of the “round” four-sphere with the same time extension).

A. Renormalized versus bare coupling constants

Before comparing CDT and FRG results let us recall how one moves between a lattice-regulated quantum field theory and the renormalized continuum quantum field theory defined from the lattice theory (assuming the continuum quantum field theory exists). This is essentially textbook stuff (see, e.g. [15]), but we feel it is useful for the following discussion to recall some details, which we have therefore collected in an Appendix. Here we just emphasize the following: the lattice theory comes with a UV cut-off a , the length of the lattice links. We denote the coupling constants used to define the lattice theory by the bare coupling constants. The existence of a renormalized continuum theory usually requires that there exists a subset of bare lattice coupling constants, a so-called critical surface, where a correlation length ξ is infinite, measured in lattice units. The renormalized coupling constants will depend on both the bare lattice coupling constants and the cut-off. By fine-tuning the bare coupling constants toward the critical surface in specific ways, one can achieve renormalized coupling constants that remain nontrivial in the limit as $a \rightarrow 0$.

The correlation length ξ will be defined in terms of the bare coupling constants, and let us for simplicity replace one of the bare coupling constants (typically the bare mass term) by ξ , and when we next talk about the bare coupling constants, we mean the remaining bare coupling constants. The critical surface will then be obtained by $\xi^{-1} \rightarrow 0$. Usually one can then relate the UV cut-off a to ξ by insisting that

$$\xi a = \ell_{\text{phys}} \quad (19)$$

represents a physical length scale (the physical correlation length) that is kept fixed. If that is the case, taking $\xi^{-1} \rightarrow 0$ becomes equivalent to taking $a \rightarrow 0$.

We can now take two different limits

- 1) One can keep the bare lattice coupling constants fixed and take the correlation length ξ to infinity. In that limit the renormalized coupling constants, which depend on both the bare coupling constants and the correlation length, will flow to an IR fixed point of the renormalized theory.
- 2) Alternatively, one can keep the renormalized coupling constants fixed when taking the correlation length to infinity. This will in general only be possible if we adjust the bare coupling constants, and in this way they become functions of the correlation length (and the fixed renormalized coupling constants) and when $\xi \rightarrow \infty$ the bare lattice coupling constants will flow to a lattice UV fixed point.

The scenario above assumes that the lattice considered is infinite since it is $\xi = \infty$ on a critical surface. In lattice field theory MC simulations will be instead performed on a finite lattice with $N = L^d$ number of lattice sites where L denotes the linear extension of the lattice and d the dimension of spacetime. $\xi = \infty$ is then replaced by $\xi \propto N^{1/d}$, since the correlation length cannot exceed the linear dimension of the lattice. In lattice field theory this leads to the concept of a pseudo-critical surface in the coupling constant space, a surface that will approach the critical surface for $N \rightarrow \infty$, and to the theory of finite-size scaling, where scaling behavior of observables when one approaches the critical surface can be extracted by studying the behavior of the observables at the pseudo-critical points, as a function of N (as discussed in the appendix). In the above discussion, the correlation length ξ is related to some matter fields living on the lattice sites, and its only relation to the lattice volume N is by various finite-size effects, for example, $\xi_{\text{max}} \propto N^{1/d}$. In quantum gravity the situation is different since the volume of spacetime V_d (or the lattice spacetime volume N) is a dynamical variable, and the way we have encountered finite-size scaling in (15)-(18) for variables $\langle N_3(t) \rangle_{N_4}$ and $\langle N_3(t)N_3(t') \rangle_{N_4}$ is slightly different: $N_4^{1/4}$ is (essentially) the correlation length. An appropriate question is then: the correlation length of what? The answer is: the correlation between spacetime points separated by a geodesic distance n in the triangulation. This can be seen explicitly in two-dimensional quantum gravity where the various 2d lattice models of quantum gravity can be solved analytically [16–18]. Let μ denote the lattice cosmological constant, μ_c its critical value, and N_2 the number of triangles in a 2d triangulation. One has

$$\langle N_2 \rangle \propto \frac{1}{\mu_c - \mu}, \quad P_\mu(n) \propto e^{-n/\langle N_2 \rangle^{1/d_h}} \quad \text{for } n > \langle N_2 \rangle^{1/d_h}. \quad (20)$$

Here d_h denotes the Hausdorff dimension of the 2d lattice gravity model and $P_\mu(n)$ the probability for two marked points to be separated by a geodesic distance n in the statistical ensemble of triangulations with cosmological constant μ . It can be seen that $\langle N_2 \rangle^{1/d_h}$ is the correlation length and goes to infinity as $\mu \rightarrow \mu_c$, the critical value of the cosmological coupling constant. The relation between the two-point function where the cosmological constant μ is fixed and the one where its conjugate variable, the two-volume N_2 , is fixed, is given by a Laplace transformation

$$P_\mu(n) = \sum_{N_2} e^{-(\mu - \mu_c)N_2} P_{N_2}(n), \quad \text{i.e.} \quad P_{N_2}(n) \propto \frac{1}{N_2^{1/d_h}} F\left(\frac{n}{N_2^{1/d_h}}\right) \quad (21)$$

for N_2 sufficiently large, so that the discretization effects are small. The point we want to emphasize is the appearance of the scaling function $F(x)$, $x = n/N_2^{1/d_h}$ for a fixed, large N_2 . It is a consequence of the divergence of the correlation length $\langle N_2 \rangle^{1/d_h}$ for $\mu \rightarrow \mu_c$, and for sufficiently large N_2 we can identify $N_2 \approx \langle N_2 \rangle$ and N_2^{1/d_h} with the correlation length. In 4d CDT we have a finite volume, since N_4 is always finite in the computer simulations. However, we observe that finite-size scaling works very well [14, 19, 20], and the measurements of $\langle N_3(t) \rangle_{N_4}$ and $\langle N_3(t)N_3(t') \rangle_{N_4}$ lead to finite-size scaling functions $F(x)$ as shown, e.g., in (16)–(17). In fact, as discussed in detail in [21], the correlation function $\langle N_3(t)N_3(t') \rangle_{N_4}$ is precisely the two-point correlator integrated over two spatial hyperplanes separated by a geodesic distance proportional to $|t - t'|$, a setup closely analogous to the setup used to measure the correlation length of a scalar field in a ϕ^4 theory on a lattice [15].

Since the Hausdorff dimension of four-dimensional CDT is four [19], it is then natural to assume that we have a correlation length $\xi \propto N_4^{1/4}$ and in this case the relation between the continuum four-volume V_4 and the lattice volume N_4 becomes similar to (19)

$$N_4 a^4 \propto V_4, \quad \text{i.e.} \quad \xi a \propto \ell_{\text{phys}} = V_4^{1/4}, \quad (22)$$

We want to apply 1) and 2) to CDT, with ξ being $N_4^{1/4}$ and the bare couplings being κ_0 and Δ , and the critical surface being $N_4 \rightarrow \infty$. For fixed κ_0 and Δ we then expect the renormalized coupling constants (which we have not yet defined) to flow to an IR fixed point. Similarly, keeping the renormalized coupling constants fixed, the bare coupling constants κ_0, Δ should flow to a lattice UV fixed point (provided it exists). We will discuss this in detail below.

B. The infrared limit

We want to compare the lattice results (16) and (17) with the FRG results (8) and (9), where in formulas (16) and (17) the lattice coupling constants Γ and δ are functions of the bare lattice coupling constants κ_0 and Δ .⁷ Let us for the moment ignore that $\delta \neq \delta_0$. Then it is natural to identify

$$\frac{\sqrt{N_4}}{\Gamma(\kappa_0, \Delta, N_4)} = \frac{\sqrt{V_4(k)}}{24\pi G_k} \simeq \frac{1}{1.63 \lambda_k g_k}. \quad (23)$$

The equation provides us with a mapping from the bare lattice couplings κ_0, Δ, N_4 to the renormalized running coupling constant $\lambda_k g_k$ that we then view as a renormalized lattice constant combination. As long as we keep the bare lattice coupling constants κ_0 and Δ fixed, Γ will essentially stay fixed for sufficiently large N_4 . As discussed above we view $N_4^{1/4}$ as proportional to a correlation length ξ . Approaching the critical surface $N_4^{-1} = 0$ should thus lead to a flow of the renormalized coupling combination to an IR fixed point, and we see that this IR fixed point should be one where $\lambda_k g_k \rightarrow 0$. Let us now check if this agrees with the IR limit obtained from FRG for $k \rightarrow 0$.

If we assume that both λ_k and g_k are small, then we are close the Gaussian fixed point of the renormalization group flow and lowest order perturbation theory yields (e.g. see the linear approximation to Eq. (74) in [4]):

$$g_k = g_{k_0} \frac{k^2}{k_0^2}, \quad \lambda_k = \left(\lambda_{k_0} - \frac{g_{k_0}}{8\pi} \right) \frac{k_0^2}{k^2} + \frac{g_{k_0}}{8\pi} \frac{k^2}{k_0^2}, \quad k \approx k_0, \quad g_{k_0}, \lambda_{k_0} \ll 1. \quad (24)$$

When $k \rightarrow 0$ one has $\lambda_k \rightarrow \infty$ unless $g_{k_0} = 8\pi \lambda_{k_0}$, in which case we start out precisely at the unique renormalization trajectory that leads to the Gaussian fixed point. Unless that is the case, lowest order perturbation theory will become invalid for $k \rightarrow 0$, since $\lambda_k \rightarrow \infty$. In most FRG approaches, the β -functions become singular when $\lambda_k = 1/2$, and this happens for finite k . An improved FRG treatment (that goes far beyond the simple Ansatz (1)) has led to the following limit for $k \rightarrow 0$ [23]:

$$g_k \propto \frac{k^2}{k_0^2}, \quad \lambda_k \propto \frac{k_0^2}{k^2}, \quad \text{for } k \rightarrow 0, \quad (25)$$

despite the fact that $\lambda_k \rightarrow \infty$ for $k \rightarrow 0$. This limit then serves as an IR fixed point in the sense that it corresponds to finite values of the dimensionful gravitational and the cosmological constants: $\Lambda_{k=0} \approx \Lambda_{k_0}$ and $G_{k=0} \approx G_{k_0}$ in the limit $k \rightarrow 0$. Eqs. (25) also imply that $g_k \lambda_k = G_k \Lambda_k > 0$ for $k \rightarrow 0$ and is therefore not compatible with the large N_4 limit of (23). If one wants an infrared limit like (25) one has to change the bare coupling constants of the lattice theory such that $\Gamma(\kappa_0, \Delta) \propto \sqrt{N_4}$ in the relation (23), a change that should not be needed in order to approach the IR fixed point, as discussed in the Appendix. However, we will discuss the $\Gamma(\kappa_0, \Delta) \propto \sqrt{N_4}$ behavior later in detail, since it is the same behavior that is needed to reach a UV fixed point.

However, in a recent paper [24] the $k \rightarrow 0$ limit has been studied using FRG for time-foliated spacetimes, a setup that is closer to our CDT approach and a new IR fixed point was found:

$$(g_k, \lambda_k) \rightarrow \left(0, \frac{1}{2} \right) \quad \text{for } k \rightarrow 0. \quad (26)$$

⁷ A first such comparison was done in [22]. However, at that time the so-called bifurcation phase C_b had not yet been discovered. It was viewed as part of phase C_{dS} .

More precisely it was found that

$$g_k \propto \frac{k^4}{k_0^4}, \quad \lambda_k - \frac{1}{2} \propto \frac{k}{k_0}, \quad \text{for } k \rightarrow 0. \quad (27)$$

Except for the unique path from the UV fixed point to the Gaussian fixed point, the paths from the UV fixed point (corresponding to $k = \infty$) will all converge to this IR fixed point for $k \rightarrow 0$. When approaching the fixed point, we have $g_k \lambda_k \rightarrow 0$. This is then compatible with the CDT limit for $N_4 \rightarrow \infty$ and κ_0, Δ fixed. This IR fixed point is different from the Gaussian fixed point since the approach to the Gaussian fixed point can be parametrized by a classical gravitational coupling constant $g_k/k^2 = G_k \rightarrow G_0$, while $\Lambda_k \rightarrow 0$ as k^2 . For the IR fixed point we have $G_k \propto k^2 \rightarrow 0$, and also $\Lambda_k \propto k^2 \rightarrow 0$. As we will now argue, this different scaling has implications for the scaling of the lattice cut-off a .

First we remark that (22) and (23) lead to further identification

$$\Gamma a^2 \propto G_k. \quad (28)$$

In the case of the Gaussian fixed point, we can write $G_k = G_0$ for small k and define the Planck length as $l_p = \sqrt{G_0}$. Thus (28) becomes

$$a \propto \frac{l_p}{\sqrt{\Gamma}} \quad \text{for } N_4 \rightarrow \infty. \quad (29)$$

Since for fixed bare lattice coupling constants κ_0, Δ , the measured $\Gamma(\kappa_0, \Delta, N_4)$ goes to a constant for $N_4 \rightarrow \infty$, we see that the UV cut-off a is of the order of the Planck length l_p , and it does not go to zero at the Gaussian fixed point. In the interior of the C_{ds} phase where Γ is bounded we reach the interesting conclusion that we cannot take the cut-off (much) below the Planck scale when approaching the Gaussian fixed point. We thus have a situation where (19) is not really valid in the sense that when approaching an IR fixed point in the renormalized coupling constants, we cannot maintain ℓ_{phys} as a constant. Eq. (22) is of course still valid, but $\ell_{\text{phys}} = V_4^{1/4}(k) \rightarrow \infty$ for $k \rightarrow 0$ since $V_4(k) \propto 1/\Lambda_k^2$ and $\Lambda_k \rightarrow 0$ at the Gaussian fixed point, so in this case (22) can be satisfied for $a = \text{const.}$ and $\xi \rightarrow \infty$.

The situation is different when approaching the IR fixed point (27), since we in that case have $G_k \propto k^2$, and we obtain from (28)

$$a \propto \sqrt{\frac{g_{k_0}}{\Gamma}} \frac{k}{k_0^2}, \quad \frac{g_{k_0}}{k_0^4} \approx \text{const.} \quad \text{for } k_0 \rightarrow 0. \quad (30)$$

Thus, $a \rightarrow 0$ for $k \rightarrow 0$. So in this case, we obtain a simple continuum limit at the IR fixed point. However, the continuum theory determined by the FRG is in some sense a trivial theory since both G_0 and Λ_0 are zero.

For future reference let us note that close to the Gaussian fixed point (24) and the IR fixed point (27) we have what can be considered as the leading contribution to the renormalization group equation for $\lambda_k g_k$ for $k \rightarrow 0$:

$$k \frac{d}{dk} (\lambda_k g_k) = 4(\lambda_k g_k) + O(k^5) \quad \text{for } k \rightarrow 0. \quad (31)$$

C. The ultraviolet limit

We are of course more interested in the UV fixed point. Following 2) (and the discussion in the Appendix) we can locate a lattice UV fixed point by keeping the renormalized couplings fixed while approaching the critical surface, i.e. while following a path in the κ_0, Δ coupling constant space where the correlation length $N_4^{1/4} \rightarrow \infty$. The relation (23) allows us to view $\lambda_k g_k$ as a combination of renormalized coupling constants also on the lattice. In the FRG approach this renormalized coupling is a running coupling, taking values between its IR and UV values.⁸ In relation (23), picking any value of κ_0, Δ, N_4 will then (in principle) correspond to a value of $\lambda_k g_k$ between its IR value and its UV value. We are then instructed to take $N_4 \rightarrow \infty$ while at the same time changing κ_0 and Δ so that $\lambda_k g_k$ stays fixed. The path followed in the κ_0, Δ plane will then lead us to the lattice UV point, provided that it exists. This flow in the lattice coupling constants is not directly related to k -flow of the renormalized coupling. As explained in the

⁸ In most FRG approaches one has a coupled set of RG equations for λ_k and g_k . However, in [12] it was possible to derive a closed FRG equation for $\lambda_k g_k$ and the β -function for $\lambda_k g_k$ has both an IR fixed point, $\lambda_0 g_0 = 0$, for $k \rightarrow 0$, and an UV fixed point $\lambda^* g^*$ for $k \rightarrow \infty$.

Appendix one should be able to reconstruct the flow of the renormalized $\lambda_k g_k$ (as a function of the correlation length $\xi = N_4^{1/4}$) by considering the whole family of flows to the UV fixed point, starting from different κ_0, Δ, N_4 . However, here we will only be interested in locating the UV fixed point and finding the critical exponents, as described in the Appendix.

According to the discussion above, we have to require

$$\frac{\sqrt{N_4}}{\Gamma(\kappa_0, \Delta, N_4)} = \text{constant} \quad \text{for } N_4 \rightarrow \infty, \quad (32)$$

in order to approach a lattice UV fixed point. For fixed κ_0, Δ in the interior of the C_{ds} phase $\Gamma(\kappa_0, \Delta, N_4)$ stays finite for $N_4 \rightarrow \infty$. Thus, a path $N_4 \rightarrow (\kappa_0(N_4), \Delta(N_4))$ in the κ_0, Δ coupling constant plane where $\Gamma(\kappa_0(N_4), \Delta(N_4), N_4) \rightarrow \infty$ for $N_4 \rightarrow \infty$ will take us to the phase boundaries of the C_{ds} region. There are three phase transition lines, the $C_b - C_{\text{ds}}$ transition line, the $B - C_{\text{ds}}$ transition line, and the $A - C_{\text{ds}}$ transition line. As we will discuss in the numerical Section below, only at the $A - C_{\text{ds}}$ transition line Γ diverges. We conclude that a putative UV fixed point has to be located along this line and could even be a UV transition line.

In earlier work we have classified the $A - C_{\text{ds}}$ transition line as a first order transition line [20, 25]. However, this has been based on the study of certain local order parameters. The usual paradigm for a first order transition associated with a matter field is that when the lattice size of system is infinite (N_4 infinite in our case) the correlation length ξ associated with the matter field will stay finite even when we approach the phase transition line. This situation cannot be realized when we associate the correlation length with $N_4^{1/4}$ and take $N_4 \rightarrow \infty$. The situation is thus more complicated for phase transition lines bordering the C_{ds} phase, and we will address this further below.

Before turning to the numerical results, we have to deal with the fact that in general δ in (17) will be different from δ_0 in (6).

D. Dealing with $\delta \neq \delta_0$

We now need to be more precise when comparing CDT lattice results with the FRG results. Let us first note that the signs of the actions in Eqs. (8) and (17) are opposite. Although CDT rotates to an Euclidean signature, the requirement of convergence of the path integral (i.e. convergence of the sum of triangulations with the appropriate Boltzmann weight) also modifies the way the conformal factor will appear (see [1] for a discussion), resulting in the sign change. In fact the minisuperspace action (17) is precisely the Hartle-Hawking minisuperspace action after the rotation of the conformal factor. In this sense the sign difference is natural. Secondly, the measured values of ω in the lattice simulations are in general different from the value ω_0 dictated by GR. In [22] we tried to fit it into the framework of Horava-Lifshitz gravity [26]. Here we will be more conservative and try to fit our data to GR represented by (6). Since we explicitly break the symmetry between space and time in our lattice regularization, we also have the freedom to scale space-like links and time-like links differently in order to obtain continuum results compatible with the spacetime symmetry present in GR. Denote the length of the time-like links by a_t and the length of the space-like links by $a_s \equiv a$. The continuum three-volume of a spatial slice at time t_i , consisting of $N_3(t_i)$ tetrahedra will then be $V_3(t_i) \propto N_3(t_i)a^3$. Similarly, the continuum four-volumes of N_4 four-simplices will be $V_4 \propto N_4 a_t a^3$. Strictly speaking the situation is somewhat more complicated for the four-simplices⁹. However, for notational simplicity we will simply write

$$V_4 = N_4 a_t a^3, \quad V_3 = N_3 a^3. \quad (34)$$

Next, introducing V_3 and V_4 we can now write (18) as

$$S = \frac{1}{\Gamma} \sum_i \left(\frac{(N_3(t_i + a_t) - N_3(t_i))^2}{N_3(t_i)} + \delta N_3^{1/3}(t_i) \right) \quad (t_i \equiv a_t i) \quad (35)$$

$$= \frac{a_t}{a^3 \Gamma} \sum_i a_t \left(\frac{(V_3(t_i + a_t) - V_3(t_i))^2 / a_t^2}{V_3(t_i)} + \frac{a^2}{a_t^2} \delta V_3^{1/3}(t_i) \right), \quad (36)$$

$$\rightarrow \frac{1}{24\pi G} \int dt \left(\frac{\dot{V}_3^2}{V_3} + \tilde{\delta} V_3^{1/3} \right), \quad \tilde{\delta} = \frac{a^2}{a_t^2} \delta, \quad 24\pi G = \frac{a^3}{a_t} \Gamma, \quad (37)$$

⁹ To be more precise, the change of V_4 is as follows (see [1] for a detailed discussion of the change of the volumes of the two kind of four-simplices mentioned in footnote 6, when the relative length of a_s and a_t are $a_t^2 = \alpha a_s^2$): the four-volume of a simplex with side length a changes from $\sqrt{5}/96 \cdot a^4$ to

$$V_4^{(1,4)} = \frac{a_t a_s^3}{96} \sqrt{8 - \frac{3}{\alpha}}, \quad V_4^{(2,3)} = \frac{\alpha_t a_s^3}{96} \sqrt{12 - \frac{7}{\alpha}} \quad (33)$$

However, we will mainly be interested in the behavior in regions of coupling constant space where ω/ω_0 is significantly smaller than 1, i.e. according to (39) α much larger than 1, and then (34) will be good enough for our discussion.

and

$$\sum_i N_3(i) = N_4 \rightarrow \int dt V_3(t) = V_4, \quad V_4 = a_t a^3 N_4. \quad (38)$$

where $\tilde{\delta}$ and ω are related as in (16): $\tilde{\delta} \omega^{8/3} = \delta_0 \omega_0^{8/3}$. If $\omega \neq \omega_0$ then $\tilde{\delta} \neq \delta_0$. On the lattice the “deformed” spheres arise because there are “too many” N_3 ’s compared to the time extension $N_t = \omega N_4^{1/4}$ measured. We can fix that by adjusting a_t such that the continuum, physical time length $N_t a_t$ agrees with the spatial extent $N_3^{1/3} a$, where we write $N_4 = N_t N_3$. From these equations we find

$$a_t = \left(\frac{\omega_0}{\omega} \right)^{4/3} a, \quad (39)$$

where we have adjusted the various constants entering in the estimate such that $a_t = a$ if $\omega = \omega_0$, the value for the geometry of a round S^4 . From Eq. (37) it then also follows that $\tilde{\delta} = \delta_0$ for the round S^4 and thus this choice of a_t leads to an action S given in (8) that we can identify with the FRG effective action for some value of the scale parameter k .

So given computer data N_4, ω, Γ we can associate a corresponding continuum, round S^4 with four-volume V_4 and gravitation constant G via:

$$(N_4, \omega, \Gamma) \rightarrow (V_4(k), \omega_0, G_k), \quad (40)$$

where

$$V_4(k) = \left(\frac{\omega_0}{\omega} \right)^{4/3} N_4 a^4, \quad 24\pi G_k = \left(\frac{\omega}{\omega_0} \right)^{4/3} \Gamma a^2 \quad (41)$$

and in particular

$$\frac{\sqrt{N_4}}{\Gamma} = \frac{\omega^2}{\omega_0^2} \frac{\sqrt{V_4(k)}}{24\pi G_k} \quad \text{or} \quad \frac{\omega^2 \Gamma(\kappa_0, \Delta, N_4)}{\omega_0^2 \sqrt{N_4}} \simeq 1.63 \lambda_k g_k. \quad (42)$$

As mentioned, the only way we can influence the values of ω and Γ is by choosing the bare lattice coupling constants κ_0 and Δ . Both ω and Γ depend only weakly on N_4 for sufficiently large N_4 . We find numerically for all the bare lattice coupling constants in phase C_{dS} that $\omega^2 \Gamma$ is bounded except close to the $A - C_{\text{dS}}$ transition. In particular, at the $C_b - C_{\text{dS}}$ transition line, which is a second order transition line [27, 28], it seems that $\omega^2 \Gamma$ stays bounded and different from zero. There might be huge finite-size effects at this second order phase transition line, since we have good reasons to believe that $\omega = 0$ deep into the C_b phase, but we do not observe any dip of ω close to the transition line. Similarly, there are large finite-size effects at the little stretch of the $B - C_{\text{dS}}$ transition, which is probably also a second order phase transition line. On the other hand, the situation at the $A - C_{\text{dS}}$ transition is relatively clear: $\Gamma \rightarrow \infty$ and $\omega \rightarrow 0$ and, most importantly, $\omega^2 \Gamma \rightarrow \infty$ (in the limit $N_4 \rightarrow \infty$) when approaching the transition from the C_{dS} side.

IV. THE PUTATIVE UV LIMIT

A necessary condition for obtaining a UV limit from the lattice theory is that we, starting from a bare coupling constant point $(\kappa_0, \Delta, N_4(0))$ associated to phase C_{dS} ¹⁰ can find a path $(\kappa_0(N_4), \Delta(N_4), N_4)$ such that

$$\frac{\omega^2(\kappa_0(N_4), \Delta(N_4), N_4) \Gamma(\kappa_0(N_4), \Delta(N_4), N_4)}{\omega_0^2 \sqrt{N_4}} \simeq 1.63 \lambda_k g_k, \quad (43)$$

for some value of k and all the way to $N_4 = \infty$, as already mentioned above (Eq. (42)). As discussed in the numerical results section below, the observed dependence on Δ is weak in the region of interest, and for notational simplicity, we will omit references to Δ in the following.

¹⁰ By that we mean that keeping κ_0 and Δ fixed and taking $N_4 \rightarrow \infty$ we end up in phase C_{dS} , what is strictly speaking only defined for $N_4 = \infty$.

As discussed in the Appendix we assume that at the critical surface, i.e. the $N_4 = \infty$ surface, we have the following behavior of $\Gamma(\kappa_0)$ and $\omega(\kappa_0)$ close to the critical point κ_0^{UV} of the $A - C_{\text{dS}}$ transition:

$$\Gamma(\kappa_0) \propto \frac{1}{|\kappa_0^{\text{UV}} - \kappa_0|^\alpha}, \quad \omega(\kappa_0) \propto |\kappa_0^{\text{UV}} - \kappa_0|^\beta, \quad \omega^2(\kappa_0)\Gamma(\kappa_0) \propto \frac{1}{|\kappa_0^{\text{UV}} - \kappa_0|^{\alpha-2\beta}}, \quad (44)$$

We further assume that for a finite N_4 there is a pseudo-critical point $\kappa_0^{\text{UV}}(N_4) < \kappa_0^{\text{UV}}$ where $\omega^2(\kappa_0, N_4)\Gamma(\kappa_0, N_4)$ has a maximum for fixed N_4 , and that this pseudo-critical point approaches κ_0^{UV} for $N_4 \rightarrow \infty$ as

$$\kappa_0^{\text{UV}}(N_4) = \kappa_0^{\text{UV}} - \frac{c}{N_4^{1/4\nu_{\text{UV}}}} \quad (\text{i.e. } \xi \propto \frac{1}{|\kappa_0^{\text{UV}} - \kappa_0^{\text{UV}}(\xi)|^{\nu_{\text{UV}}}}). \quad (45)$$

This implies that

$$\Gamma(\kappa_0^{\text{UV}}(N_4)) \propto N_4^{\alpha/4\nu_{\text{UV}}}, \quad \omega(\kappa_0^{\text{UV}}(N_4)) \propto N_4^{-\beta/4\nu_{\text{UV}}}, \quad (46)$$

as well as

$$\omega^2(\kappa_0^{\text{UV}}(N_4))\Gamma(\kappa_0^{\text{UV}}(N_4)) \propto N_4^{(\alpha-2\beta)/4\nu_{\text{UV}}}. \quad (47)$$

From Eq. (43) it follows that we have to have

$$\alpha - 2\beta \geq 2\nu_{\text{UV}} \quad (48)$$

and if that is the case the following path in the bare lattice coupling constant space will lead us to the putative UV fixed point while keeping $\lambda_k g_k$ fixed:

$$\kappa_0(N_4) = \kappa_0^{\text{UV}} - \frac{c}{N_4^{1/2(\alpha-2\beta)}} \quad (49)$$

Following the discussion in the Appendix, only with α there replaced by $\alpha - 2\beta$, Eq. (83) in the Appendix suggests that we should associate a critical exponent

$$\theta_{\kappa_0^{\text{UV}}} = \frac{2}{\alpha - 2\beta} \quad (50)$$

to the putative UV fixed point. Presently, it is unclear to us if this can be directly compared to the corresponding critical exponent obtained using the FRG approach. The main problem is that we do not know the precise connection between our correlation length $\xi \propto N_4^{1/4}$ used to derive $\theta_{\kappa_0^{\text{UV}}}$ and the scale factor k used in the FRG.

The MC simulations discussed in next Section indicate that we have

$$\frac{\beta}{4\nu_{\text{UV}}} \approx 0.24 \pm 0.02, \quad \frac{\alpha}{4\nu_{\text{UV}}} \approx 1.04 \pm 0.02, \quad \nu_{\text{UV}} \approx 0.21 \pm 0.03, \quad (51)$$

where we have taken the average values measured using two different methods. Clearly it would be very desirable if we could measure the exponents with larger precision, but it will require considerably larger computer simulations. In the following discussion we will assume that the actual exponents satisfy

$$\frac{\alpha - 2\beta}{4\nu_{\text{UV}}} > \frac{1}{2}, \quad \frac{\beta}{4\nu_{\text{UV}}} < \frac{1}{4}, \quad (52)$$

and let us understand better the relation between the FRG flow and what we observe on the lattice. From (41) we find, using that $\omega \propto N_4^{-\beta/4\nu_{\text{UV}}}$ and $V_4(k) \propto \Lambda_k^{-2}$, that

$$a \propto \frac{1}{\sqrt{\Lambda_k}} N_4^{-\frac{1}{4}(1+\frac{\beta}{3\nu_{\text{UV}}})}, \quad \text{i.e. } a \propto \frac{1}{k} N_4^{-\frac{1}{4}(1+\frac{\beta}{3\nu_{\text{UV}}})} \quad \text{for } k \rightarrow \infty. \quad (53)$$

Thus the lattice spacing a scales to zero for a fixed value of k when we approach the critical surface $N_4 = \infty$. From Eqs. (41) and (53) it follows that also the a_t scales to zero when approaching the critical surface, but slower:

$$a_t \propto \frac{1}{\sqrt{\Lambda_k}} N_4^{-\frac{1}{4}(1-\frac{\beta}{\nu_{\text{UV}}})} \quad \text{i.e. } a_t \propto \frac{1}{k} N_4^{-\frac{1}{4}(1-\frac{\beta}{\nu_{\text{UV}}})} \quad \text{for } k \rightarrow \infty. \quad (54)$$

This slower decrease of a_t is a reflection of the fact that we, when approaching the $A - C_{\text{DS}}$ transition line, have to rescale our increasingly “elongated” lattice four-spheres in order to match the round four-spheres of the FRG. Thus, under the assumptions stated in (52) the $A - C_{\text{DS}}$ phase transition point κ_0^{UV} can serve as a UV fixed point and approaching the fixed point we have a well-defined mapping of our deformed four-spheres to the four-spheres predicted by the simplest FRG equations all the way to the lattice UV fixed point. Recall again to the reader that this flow occurs for a fixed value of $\lambda_k g_k$. Thus, it is not directly related to the FRG flow parameter k and the flow of $\lambda_k g_k$ to its UV fixed point. However, the larger k the smaller the lattice spacing a and we see that when $k \rightarrow \infty$ then $a \rightarrow 0$ as $1/k$, simply reflecting that $V_4(k) \rightarrow 0$ as $1/k^4$.

Let us finally note that the UV critical exponent $\theta_{\kappa_0^{\text{UV}}}$, defined by Eq. (50), given the numerical values (51), will be

$$\theta_{\kappa_0^{\text{UV}}} = 4 \pm 1. \quad (55)$$

This value is larger than the one reported in [13] and much larger than the one reported in [12], but as already emphasized, we do not know the precise relation between the FRG k and our ξ . Unfortunately, Eqs. (53) and (54) do not help us, since the lattice spacing a also appears.¹¹

If Eqs. (52) are *not* satisfied it is difficult to associate a UV fixed point to the $A - C_{\text{DS}}$ phase transition, at least following the philosophy used in this article. It is of course unfortunate that the numerical results do not allow us to decide whether or not a UV fixed point is favored.

V. NUMERICAL RESULTS

In this Section, we present results of the numerical Monte Carlo (MC) simulations performed inside the de Sitter phase C_{DS} in a region of κ_0, Δ coupling constant space close to the three phase boundaries discussed above; see also Figures 1 and 2.¹² As already explained, the measured values of ω and Γ are both functions of κ_0 and Δ , but for sufficiently large systems, do not depend on N_4 (except very close to the phase boundaries, which also shift with N_4). Therefore, as a starting point, to check the dependence one can perform MC simulations for fixed N_4 . We have chosen to set¹³ $N_4^{(1,4)} = 160\,000$ and performed a series of measurements in a grid of points: $\kappa_0 = 3.0, \dots, 4.5$, $\Delta = -0.07, \dots, 0.20$, see Figure 2. In each point, we measured $\langle N_3(t) \rangle$ and $\langle N_3(t_1)N_3(t_2) \rangle$ and used these data to calculate $\omega(\kappa_0, \Delta)$ and $\Gamma(\kappa_0, \Delta)$. The values of ω were obtained by fitting $\langle N_3(t) \rangle$ to the semi-classical solution for an (elongated) four-sphere, see Eqs. (15)-(16). As in the volume profile $\langle N_3(t) \rangle$ one observes a “stalk” part, where $\langle N_3(t) \rangle \approx \text{const.}$ in some range of t , and the “blob” part, where the semiclassical solution is valid, we fitted a function¹⁴

$$\langle N_3(t) \rangle = \max \left(\text{const.}, \frac{3}{4\omega} N_4^{3/4} \cos^3 \left(\frac{t}{\omega N_4^{1/4}} \right) \right) \quad (56)$$

where const. and N_4 are free parameters and we checked that fitted values of N_4 agree with $\sum_t \langle N_3(t) \rangle$ inside the “blob”. The values of Γ were computed twofold:

- (1) by reconstructing the effective action (18) from the (connected) correlator $\langle N_3(t_1)N_3(t_2) \rangle - \langle N_3(t_1) \rangle \langle N_3(t_2) \rangle$ (for details we refer to [30, 31]), and
- (2) directly from the amplitude of fluctuations (note that the form of the effective action (18) implies Gaussian three-volume fluctuations with amplitude $\delta N_3(t) \propto \sqrt{\Gamma N_4}$).

In Fig. 3 we compare both methods of measuring Γ for fixed $\Delta = 0$ and a choice of κ_0 using four different lattice volumes $N_4^{(1,4)} = 80\,000, 160\,000, 480\,000, 720\,000$, note that the proportionality constant in method (2) is the same in all plots. It is seen that both methods agree except very close to the phase boundary, where for larger volumes the results of method (1) are visibly higher than those of the method (2). In further analysis, we decided to take the average Γ from (1) and (2).

¹¹ A further discussion of the relation between the critical exponents will appear in [29].

¹² One should note that in the previous study of this region of the parameter space [22] the existence of the bifurcation phase C_b was not known, and therefore one could not analyze all phase transition lines in a proper way. Also, because of much lower computing power, one was only able to simulate quite small triangulations (up to $N_4^{(4,1)} = 40\,000$). Now, thanks to better computer resources and improved MC algorithms, we were able to simulate much larger systems (up to $N_4^{(4,1)} = 720\,000$) and thus considerably reduce finite-size effects.

¹³ In the MC simulations we control the number of the $(1, 4)$ -simplices, see footnote 6, and the number of $(2, 3)$ -simplices adjusts dynamically. For given values of κ_0, Δ the ratio of the two types of simplices is (approximately) constant and independent of N_4 .

¹⁴ The existence of the “stalk” connecting both sides of the “blob” is due to the topological constraints of triangulations used in the MC simulations. Due to large volume fluctuations close to the $A - C_{\text{DS}}$ phase transition the volume $\sum_t \langle N_3(t) \rangle$ contained in the “stalk” is large making the volume $\sum_t \langle N_3(t) \rangle$ contained in the “blob” much smaller than total volume $N_4^{(1,4)}$.

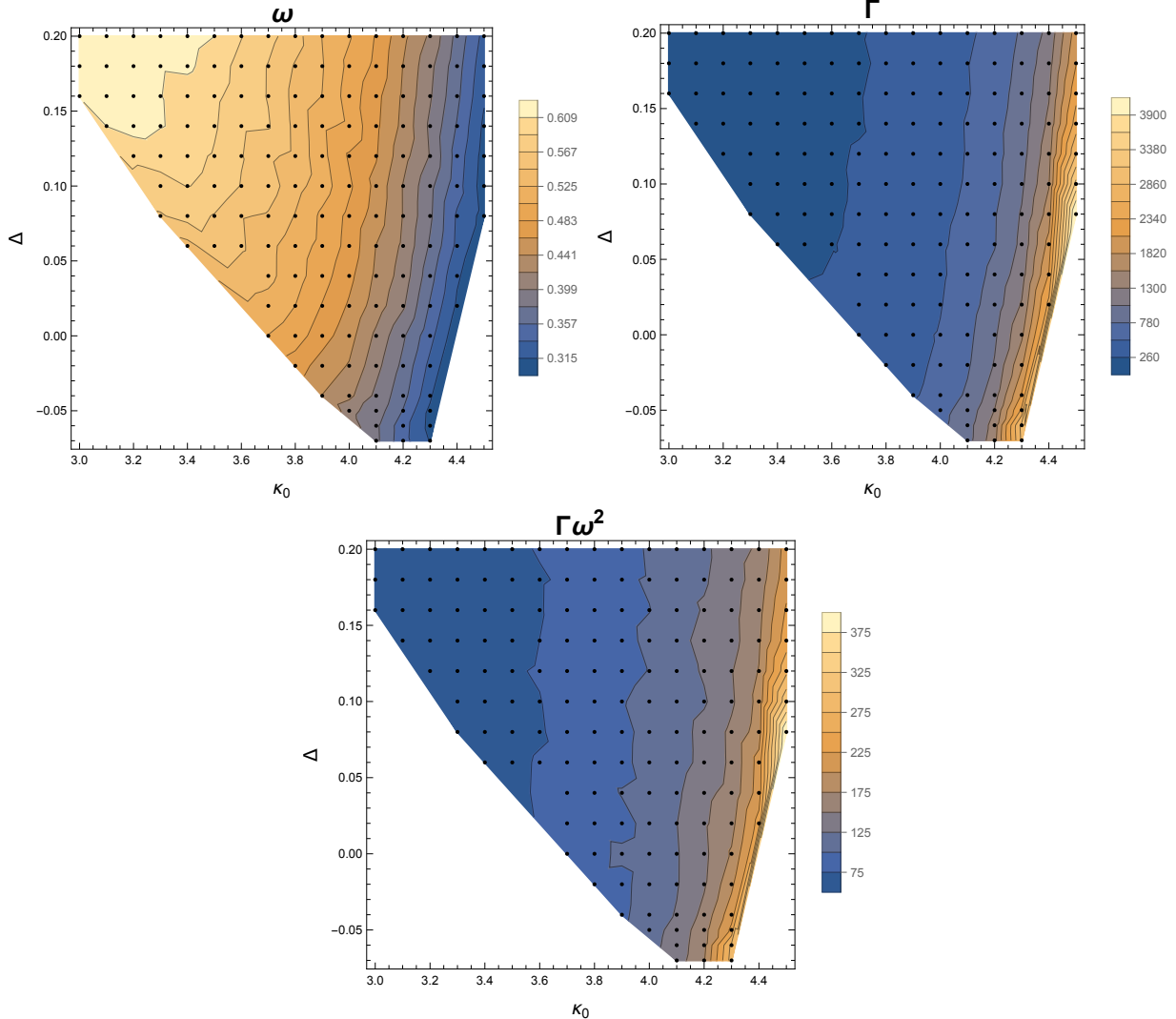


FIG. 2. Contour plots of ω (left), Γ (right) and $\Gamma\omega^2$ (bottom) in the function of the CDT coupling constants κ_0, Δ . Points where actual measurements were done are denoted as black dots in the plots.

The dependence of ω , Γ and $\Gamma\omega^2$ on κ_0, Δ for fixed $N_4^{(1,4)} = 160\,000$ is shown in Figure 2. It is seen that both ω and Γ change only slightly as a function of Δ , whereas they strongly depend on κ_0 (ω decreases with κ_0 while Γ increases with κ_0). In the study of the ultraviolet limit we are interested in a product $\omega^2\Gamma(\kappa_0, \Delta, N_4)$ which should diverge as $\sqrt{N_4}$ for $N_4 \rightarrow \infty$, see Eq. (43), and it seems that the only way to achieve this is by approaching the $A - C_{\text{ds}}$ phase transition line, where indeed $\omega^2\Gamma$ substantially grows. The non-trivial problem remains how one should move in the κ_0, Δ coupling constant space when approaching the phase transition. Since, as seen in Fig. 2 (bottom), $\omega^2\Gamma$ is almost independent of Δ and grows with κ_0 , we have chosen the simplest possible way by fixing Δ and only changing $\kappa_0 \rightarrow \kappa_0^{\text{UV}}(N_4)$. In the following, we provide evidence that this conjecture may indeed be correct.

To investigate this in detail, we performed a series of precise MC measurements for fixed $\Delta = 0$ and a dense grid of κ_0 using a set of lattice volumes $N_4^{(4,1)} = 40\,000, 80\,000, 160\,000, 200\,000, 480\,000, 720\,000$. In Figure 4 we plot the measured values of ω , Γ and $\omega^2\Gamma$. It is seen that indeed well inside phase C_{ds} the behavior is independent of N_4 , as it should be if the semiclassical solution (15)-(16) and the effective action (17) hold, but very close to the phase boundary the measured values of $\omega^2\Gamma$ diverge more and more with increasing N_4 . Note that, as discussed in previous sections and in the Appendix, the position of pseudo-critical points also moves with N_4 and only in the limit $N_4 \rightarrow \infty$ one recovers the true critical behavior when $\kappa_0^{\text{UV}}(N_4) \rightarrow \kappa_0^{\text{UV}}$. One can therefore measure the dependence of ω and Γ

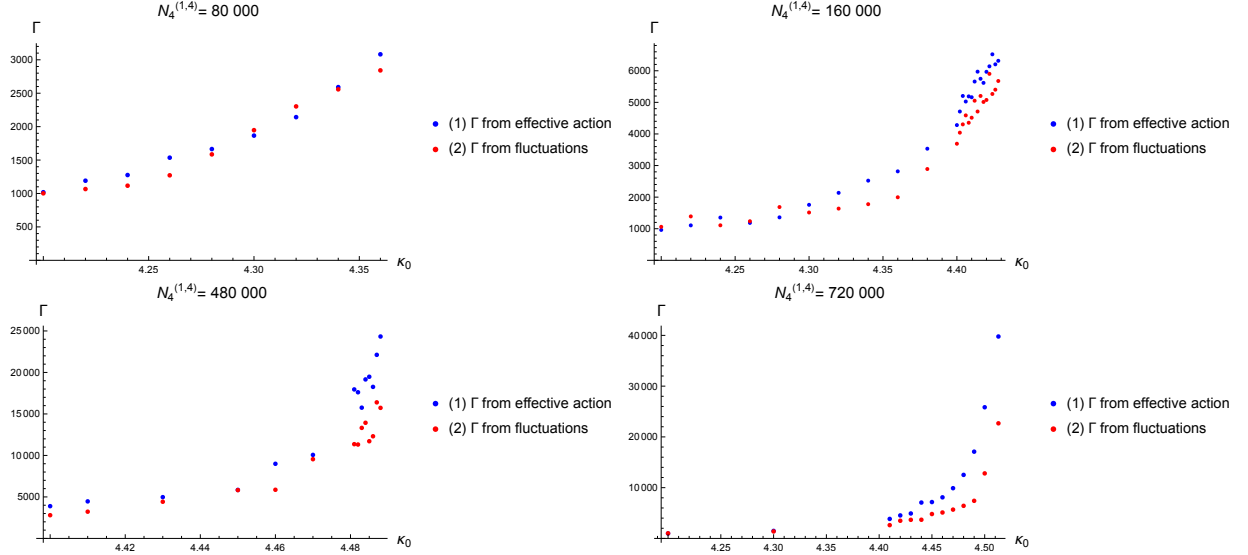


FIG. 3. Values of Γ computed using two different methods discussed in the text, measured for $\Delta = 0$ and a choice of κ_0 near the $A - C_{\text{DS}}$ transition for $N_4^{(1,4)} = 80\,000, 160\,000, 480\,000, 720\,000$.

on N_4 at (or in practice as close as one can get¹⁵) pseudo-critical points $\kappa_0^{\text{UV}}(N_4)$ and fit the critical exponents α, β and ν_{UV} from Eqs. (45)-(47). The results were summarized in Figures 5 and 6. In Fig. 5 we show the critical scaling of ω, Γ and $\omega^2\Gamma$ both as function of total lattice volume $N_4^{(1,4)}$ (left plots) and as function of N_4 volume contained in the "blob" (N_4 values fitted from Eq. (56)). The measured critical exponents from scaling with $N_4^{(1,4)}$

$$\frac{\beta}{4\nu_{\text{UV}}} = 0.25 \pm 0.02, \quad \frac{\alpha}{4\nu_{\text{UV}}} = 1.07 \pm 0.02, \quad \frac{\alpha - 2\beta}{4\nu_{\text{UV}}} = 0.58 \pm 0.04 \quad (57)$$

are a bit higher than those resulting from scaling with N_4 in the "blob"

$$\frac{\beta}{4\nu_{\text{UV}}} = 0.23 \pm 0.02, \quad \frac{\alpha}{4\nu_{\text{UV}}} = 1.00 \pm 0.02, \quad \frac{\alpha - 2\beta}{4\nu_{\text{UV}}} = 0.54 \pm 0.04 \quad (58)$$

but agree within (two) standard deviations of the fits. In Fig. 6 we plot the critical scaling of $\kappa_0^{\text{UV}}(N_4)$ at the $A - C_{\text{DS}}$ phase transition together with a fit of Eq. (45). The best fit of the critical exponent gives

$$\nu_{\text{UV}} = 0.16 \pm 0.03. \quad (59)$$

One should take this result with some caution as our earlier measurements showed that the $A - C_{\text{DS}}$ transition is a first order phase transition [20, 25] for which one may expect $\nu_{\text{UV}} = 0.25$. We have verified that for $\Delta = 0$ one still observes many signatures of the first order transition such as MC simulation tunneling between two metastable states of phase C_{DS} and phase A at pseudo-critical points. Also some hysteresis at the position of the pseudo-critical points is observed for the two largest volumes in our MC simulations, see Fig. 6 where we compare simulations initiated from inside phase C_{DS} (used above) with those initiated from inside phase A , the later data show the critical exponent

$$\nu_{\text{UV}} = 0.25 \pm 0.03 \quad (60)$$

fully consistent with a first order transition.

The finite-size scaling analysis above was based on the assumption that we keep Δ fixed ($\Delta = 0$) while changing $\kappa_0 \rightarrow \kappa_0^{\text{UV}}(N_4)$. Last but not least, one should therefore investigate the dependence of the results on the choice of Δ . We performed a series of similar measurements for $\Delta = -0.02, 0.2, 0.8$. Due to the limited computer resources in these MC simulations, we only managed to investigate a smaller set of lattice volumes $N_4^{(1,4)} = 80\,000, 160\,000, 480\,000$. In Figure 7 we plot ω and Γ measured for various Δ as a function of the (reduced) $\kappa_0/\kappa_0^{\text{UV}}(\Delta, N_4)$, note that the position of pseudo-critical points $\kappa_0^{\text{UV}}(\Delta, N_4)$ depends both on Δ and N_4 . Our conclusion is that the results are universal, independent of Δ choice¹⁶.

¹⁵ We have chosen the largest κ_0 inside phase C_{DS} for which in the MC simulations we cannot see any tunneling between phase C_{DS} and phase A .

¹⁶ These MC runs lasted much shorter than for $\Delta = 0$ case. The smaller systems with $N_4^{(1,4)} = 80\,000, 160\,000$ show very consistent results, while the data quality for the largest systems with $N_4^{(1,4)} = 480\,000$ is visibly worse.

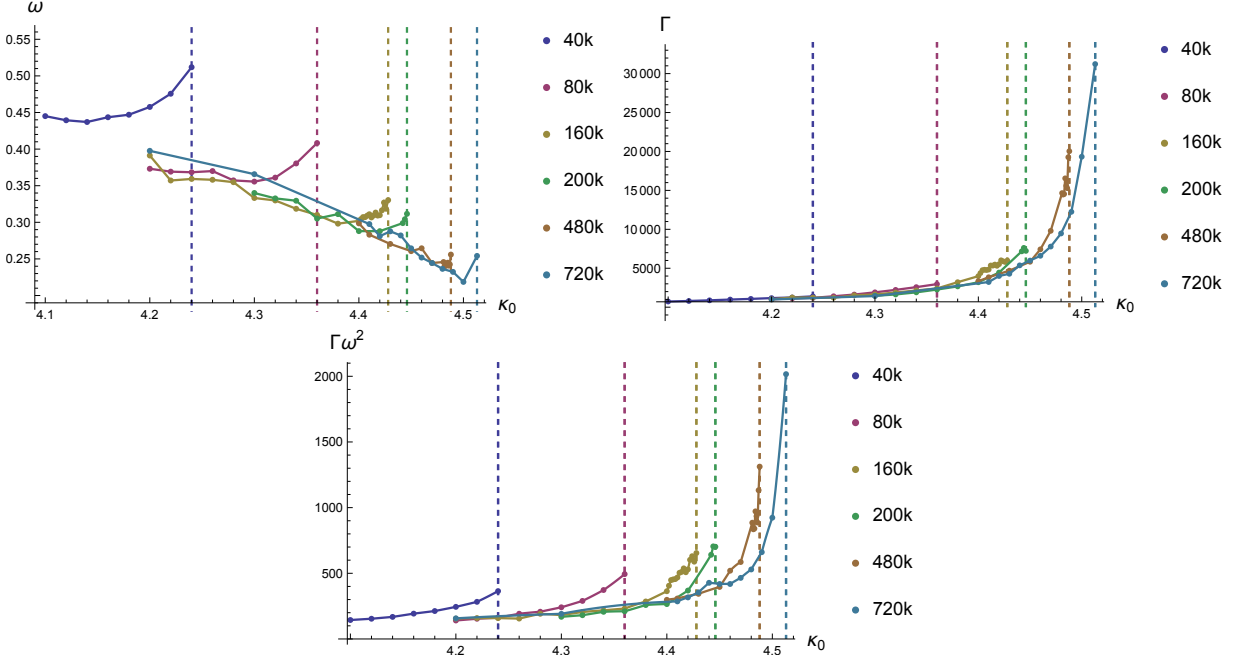


FIG. 4. Dependence of ω (left), Γ (right) and $\Gamma\omega^2$ (bottom) on κ_0 for fixed $\Delta = 0$ measured for different lattice volumes $N_4^{(4,1)} = 40\,000, 80\,000, 160\,000, 200\,000, 480\,000, 720\,000$ (denoted by different colors). Positions of κ_0 closest to the pseudo-critical points $\kappa_0^{\text{UV}}(N_4)$ are denoted by dashed lines.

VI. DISCUSSION

In this article, we have tried to relate the simplest FRG flow to the CDT effective action for the scale factor. Keeping the dimensionless lattice couplings fixed and moving towards the critical surface of the lattice theory, the renormalized coupling constants will generally flow to an infrared fixed point. Quite encouraging, we have seen a behavior that can be interpreted that way for the coupling constant $g_k \lambda_k = G_k \Lambda_k$, where G_k and Λ_k are the gravitational and the cosmological couplings used in FRG. This infrared fixed point could either be the Gaussian fixed point observed in all FRG approaches, or it could be the new IR fixed point discovered in [24]. In principle, the choice of bare CDT coupling constants could lead either to the Gaussian fixed point or to the new IR fixed point, such that we have a situation like the one illustrated in Fig. 8 in the Appendix, where there are two IR fixed points and one UV fixed point. In the FRG approach, the flow to the Gaussian fixed point is very special and the generic flow would be a flow to the IR fixed point. The present study cannot distinguish between the two fixed points. However, it should be possible to do so, since the Gaussian fixed point allows for the value of the running gravitational coupling constant G_k to be different from zero for $k \rightarrow 0$. Approaching the Gaussian fixed point, one can then have a non-trivial coupling to matter fields. That seems more difficult when approaching the IR fixed point where $G_0 = 0$. In the past, we have studied the inclusion of scalar fields in four-dimensional CDT (and also in 2d CDT [32]). In four dimensions the effect has not been large, except when there has been a non-trivial interplay between the topology of spacetime and topological properties of the scalar field [33]. The large N_4 limits of these earlier investigations have to be reassessed in order to relate them to the flow towards an IR limit.

The analysis of the RG flow to a lattice UV fixed point provided in the Appendix was based on the assumption that one knows observables that have a well defined continuum limits when one approaches the UV fixed point. In the FRG framework, such a dimensionless variable is ΛG . The FRG study, using the simplest truncation of the quantum effective action, suggests that we can relate the running renormalized coupling constant $\Lambda_k G_k$ to a similar quantity measured on the CDT lattice via Eq. (42). This led us to identify possible UV fixed points in the CDT κ_0, Δ coupling constant space as located on the $A - C_{\text{dS}}$ line. We move along the transition line mainly by increasing the coupling constant Δ (and making minor adjustments of κ_0), but the critical behavior seems to be quite independent of Δ along the transition line. This is why we dropped any reference to Δ when discussing the approach to the $A - C_{\text{dS}}$ line in the former Section. Keeping Δ fixed, we will approach the critical point $\kappa_0^{\text{UV}}(\Delta)$ of the $A - C_{\text{dS}}$ line when following the pseudo-critical point $\kappa_0^{\text{UV}}(\Delta, N_4)$, taking $N_4 \rightarrow \infty$. It is somewhat remarkable that following this pseudo-critical line $\omega^2 \Gamma$ scales approximately like $\sqrt{N_4}$, since ω and Γ both scale quite differently and non-trivially when following

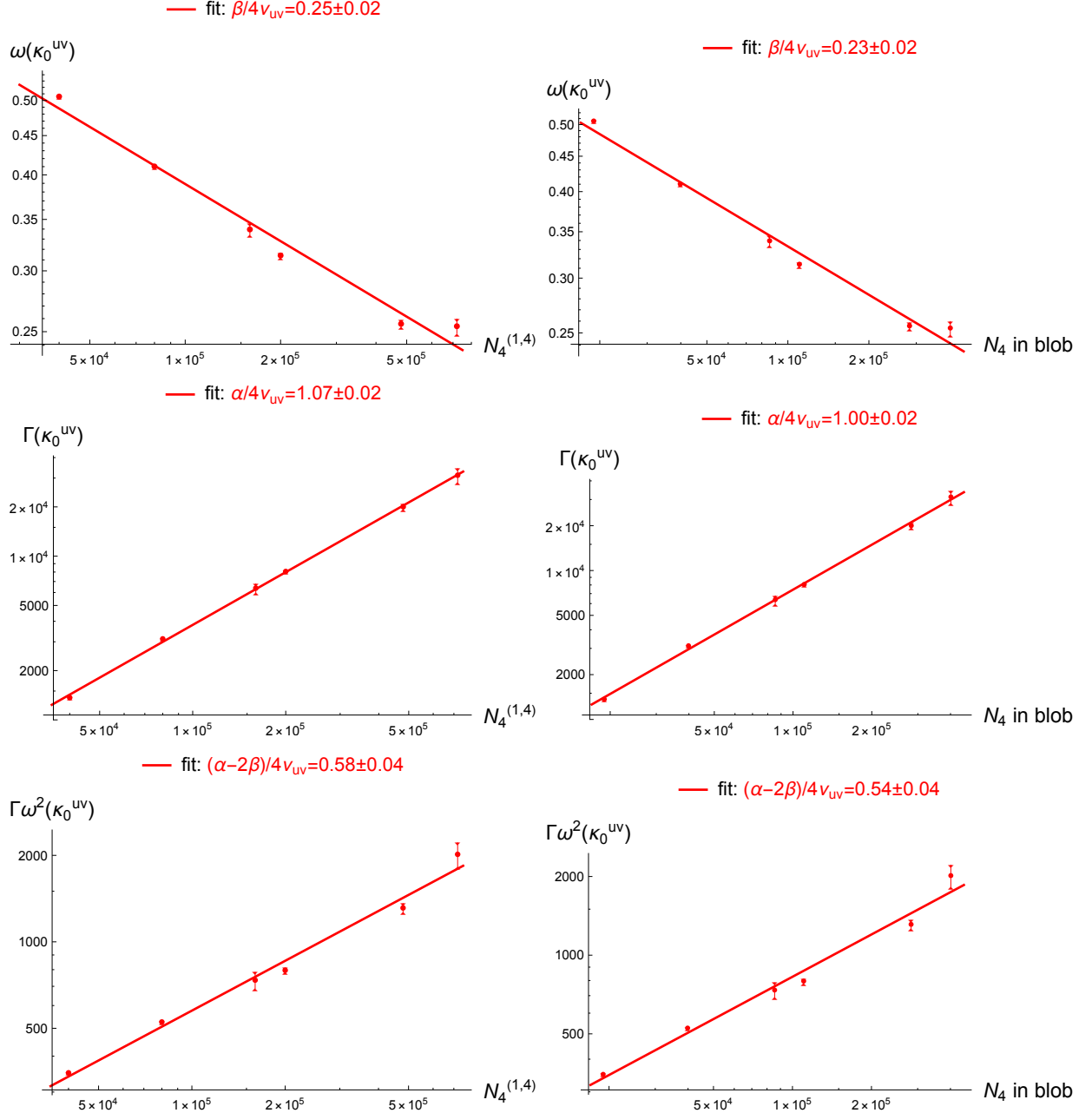


FIG. 5. Critical scaling of ω (top), Γ (middle) and $\Gamma\omega^2$ (bottom) measured closest to the pseudo-critical points $\kappa_0^{\text{UV}}(N_4)$ (see Fig. 4) for fixed $\Delta = 0$. Fits of Eqs. (46)-(47) are depicted by solid lines. Left figures show scaling in the function of the total lattice volume $N_4^{(1,4)}$, right figures show scaling in the function of the N_4 volume contained in the "blob". Note the log-log scale in all plots.

$\kappa_0^{\text{UV}}(\Delta, N_4)$. This would also imply that $\kappa_0^{\text{UV}}(\Delta)$ is indeed a candidate for a UV fixed point. However, the present accuracy of our data does not allow us to claim with certainty that $\omega^2\Gamma$ scales this way, and as discussed in the last Section, such a scaling is not needed in order to view $\kappa_0^{\text{UV}}(\Delta)$ as a UV fixed point. What is needed is that $\omega^2\Gamma$ scales with a power N_4^γ where $\gamma \geq \frac{1}{2}$. If $\gamma > \frac{1}{2}$ one will be able to verify this with sufficient computer resources. Alternatively, if we eventually will find that $\gamma < \frac{1}{2}$ along the pseudo-critical line we would have to conclude that κ_0^{UV} is not a UV fixed point and we would have the ϕ^4 situation discussed in the Appendix: we have a critical surface, but it is only associated with an IR fixed point.

The last point we would like to emphasize is the interpretation of $N_4^{1/4}$ as a correlation length that diverges as

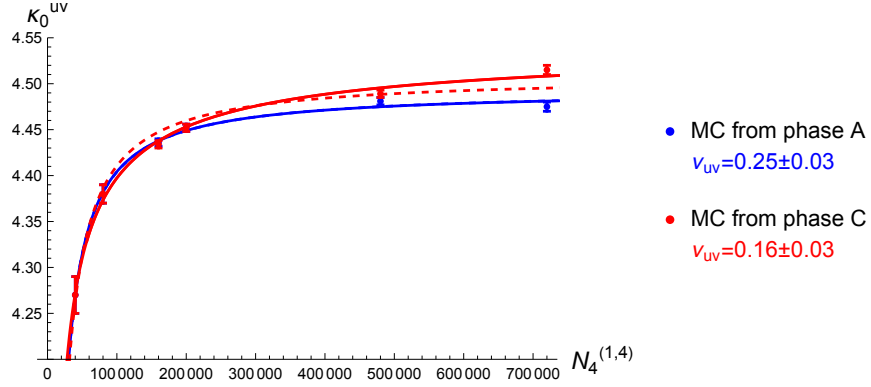


FIG. 6. Critical scaling of $\kappa_0^{\text{UV}}(N_4)$ at the $A - C_{\text{ds}}$ phase transition. MC simulations initiated from inside phase C are plotted in red and those initiated from inside phase are A in blue. For the two largest volumes hysteresis is clearly visible. Solid lines are fits of Eq. (45) including the critical exponent ν_{UV} as a free parameter. For comparison we also plot as dashed lines the fits with fixed $\nu_{\text{UV}} = 0.25$ which should be expected at a first order phase transition.

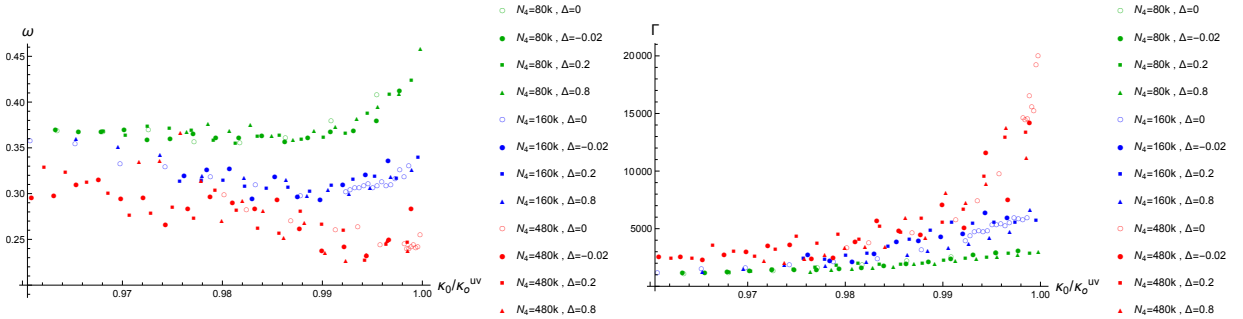


FIG. 7. Universal behavior of ω (left) and Γ (right) as a function of the (reduced) $\kappa_0/\kappa_0^{\text{UV}}(\Delta, N_4)$. Data measured for $\Delta = -0.02, 0, 0.2, 0.8$ are plotted with different markers. Colors indicate lattice volumes $N_4^{(4,1)} = 80\,000$ (green), $160\,000$ (blue) and $480\,000$ (red).

$N_4 \rightarrow \infty$. The numerical expressions for $\langle N_3(t_i) \rangle_{N_4}$ and $\langle N_3(t_i) N_3(t_j) \rangle_{N_4}$ fit perfectly with a finite-size scaling picture where one has a the correlation length ξ equal to the size of the system, here being $N_4^{1/4}$. As discussed above, the correlation length refers to a point-point correlation. Such a correlation is only non-trivial and interesting in the case where we have fluctuating geometries, i.e. in quantum gravity, and in quantum gravity it is in some sense the most elementary diffeomorphism invariant correlator one can have. It contains a wealth of information about the quantum universe, e.g. about the local and global Hausdorff dimensions of the ensemble of geometries that enters into the path integral of quantum gravity. Since this correlator is not generally appreciated let us for completeness provide the continuum definition here¹⁷:

$$G(R) = \int \mathcal{D}[g] e^{-S[g]} \iint d^4x d^4y \sqrt{g(x)} \sqrt{g(y)} 1(x) 1(y) \delta(D_g(x, y) - R), \quad (61)$$

where $D_g(x, y)$ denotes the geodesic distance between x and y , calculated using the metric g , and where $1(x)$ is the function with value 1 for all x . In the lattice formulation of quantum gravity we have in the path integral an ensemble of geometries. The (fractal) properties of this ensemble is determined by a combination of the Boltzmann weight associated to each geometry via the action, and the entropy of the geometries, i.e. the number of lattice geometries with the same action. Depending on the choice of the bare coupling constants in the (lattice) action the ensemble of geometries might or might not have interesting (fractal) properties. In the former case $G(R)$ will typically have a correlation length $\xi \propto \langle N_4 \rangle^{1/d_h}$, d_h being the Hausdorff dimension of the ensemble of geometries. Thus $\xi \rightarrow \infty$ when

¹⁷ The definition can be generalized to correlators not between points x and y , but between fields $\phi(x)$ and $\phi(y)$ by including the matter action and also integration over field configurations in the path integral and replacing $1(x)1(y)$ in (61) with $\phi(x)\phi(y)$. It would then be the correlator $\langle \phi(x)\phi(y) \rangle$ where x and y are separated a geodesic distance R , averaged over all points x, y .

$\langle N_4 \rangle \rightarrow \infty$. As we have mentioned above, this is a somewhat different kind of criticality than one usually encounters in lattice field theory, where ξ and N_4 will be independent. It is therefore not necessarily related to whether or not a phase transition (like the $A - C_{\text{dS}}$) transition is a first or second order transition when viewed in terms of some other order parameters. This is why we do not discard the $A - C_{\text{dS}}$ transition as relevant for continuum gravitation physics. Also, depending on the lattice gravity model, one can have such a scaling and a “continuum limit” that however has nothing to do with our “real world”. As an example, consider the so-called Dynamical Triangulations (DT) model where one is not imposing the time foliation present in CDT [34, 35]. The model has two coupling constants κ_0 and κ_4 , corresponding to the similar coupling constants in CDT. There is a phase transition point κ_0^c in κ_0 and for $\kappa_0 > \kappa_0^c$ one finds a so-called branched polymer phase: for a given value of $\kappa_0 > \kappa_0^c$ the statistical model becomes critical for $\kappa_4 \rightarrow \kappa_4^c(\kappa_0)$. One finds that $\langle N_4 \rangle \rightarrow \infty$ as $1/(\kappa_4 - \kappa_4^c(\kappa_0))$ and a correlation length $\xi(\kappa_4) \propto \langle N_4 \rangle^{1/2}$, determined by the exponential fall off of $G(R)$. We have a universe consisting of branched polymers with Hausdorff dimension 2, and one can take a scaling limit but it is not interesting from the point of view of representing our 4d world¹⁸. The remarkable aspect of the CDT geometries in phase C_{dS} is not that they exhibit finite-size scaling (this is also the case for the DT branched polymers), but that they look like a de Sitter universe with superimposed quantum fluctuations, and the exciting aspect of the present results is that there is a reasonable chance that the lattice theory, apart from a IR limit, also has a non-trivial UV limit.

Acknowledgments

It is a pleasure to thank Frank Saueressig for numerous enlightning discussions about FRG. We are also grateful to Renata Ferrero and Martin Reuter for discussing the physics related to the simplest FRG truncation used in this article as well as Kevin Falls and Renata Ferrero for discussions related to the critical UV exponent. We also thanks Renate Loll for a careful reading of the manuscript and corresponding constructive comments. JA thanks the Perimeter Institute for Theoretical Physics, where part of this work was completed, for hospitality and support. Research at the Perimeter Institute is supported by the Government of Canada through the Department of Innovation, Science and Economic Development and by the Province of Ontario through the Ministry of Colleges and Universities. DN is supported by the VIDI programme with project number VI.Vidi.193.048, which is financed by the Dutch Research Council (NWO). The research has been supported by a grant from the Priority Research Area (DigiWorld) under the Strategic Programme Excellence Initiative at Jagiellonian University.

APPENDIX

The ϕ^4 example

As an example of how to approach a lattice field theory UV fixed point, we consider a ϕ^4 lattice field theory in four dimensions.¹⁹ The lattice action used is

$$S = \sum_n \left(\sum_{m=1}^4 (\phi(n+m) - \phi(n))^2 + \mu_0 \phi^2(n) + \kappa_0 \phi^4(n) \right), \quad (62)$$

where the field and the coupling constants μ_0 and κ_0 are dimensionless and the length of the lattice links is 1. We assume $\kappa_0 \geq 0$. At each value of the coupling constants μ_0, κ_0 we have a correlation length $\xi(\mu_0, \kappa_0)$ of the two-point function. The lattice theory has a second order phase transition line where $\xi = \infty$. It is the phase transition line separating the symmetric phase where $\langle \phi \rangle = 0$ from the broken phase where $\langle \phi \rangle \neq 0$. We will only discuss approaching the phase transition line from the symmetric phase. Rather than using μ_0 , it is convenient to use ξ^{-1} as a variable when discussing the phase diagram. The phase transition line will then be the line $\xi^{-1} = 0$. On this phase transition line there might be UV and IR fixed points, as illustrated in Fig. 8. In a ϕ^4 theory in four dimensions, the existence of a UV fixed point would imply that there exists a renormalized ϕ^4 coupling constant $\kappa_R > 0$. This renormalized coupling constant is usually defined in a specific way in terms of correlation functions at a given momentum scale and it is an observable in the continuum renormalized quantum field theory. All renormalized observables \mathcal{O}_R in the

¹⁸ One can try to analyze the DT model by approaching the critical point κ_0^c either from the branched polymer phase or from the other side, the so-called crumpled phase and try to find non-trivial scaling, precisely like we here find non-trivial scaling when approaching the $A - C_{\text{dS}}$ transition from the C_{dS} side. This is still work in progress and also includes a study of models that enlarge the pure Einstein-Hilbert action by adding other terms (somewhat similar to the additional terms in the CDT action) [36, 37]

¹⁹ Disclaimer: the ϕ^4 theory in four dimensions has no UV fixed point, so the scenario outlined is not realized, as mentioned in the figure caption of Fig. 8. However, the fact that this scenario was not seen in a ϕ^4 theory was used in [38] to argue that there is no UV fixed point in the ϕ^4 lattice field theory.

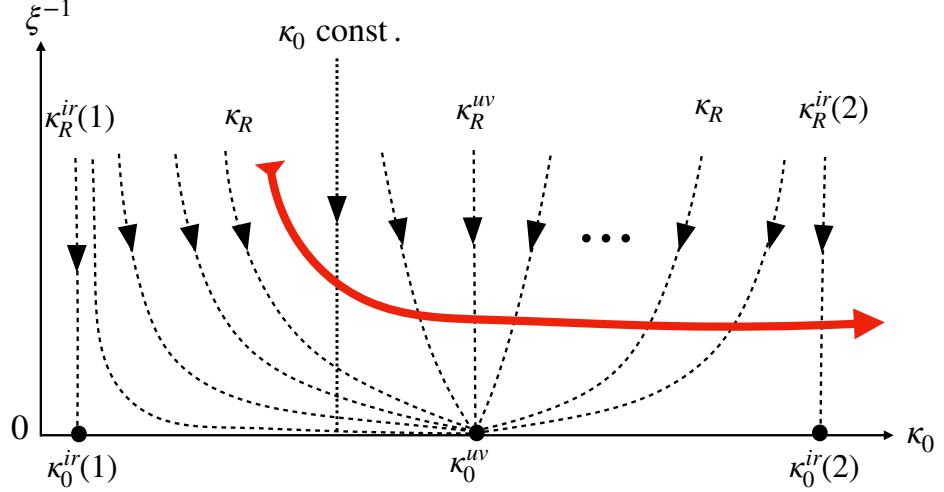


FIG. 8. The tentative ϕ^4 phase diagram with an UV fixed point and two IR fixed points. The dashed lines are paths where the renormalized ϕ^4 coupling constant κ_R is kept fixed, while on the dotted line the bare coupling constant κ_0 is fixed. The full-drawn red line illustrate the way the real renormalization group flow would be in a ϕ^4 theory with a fixed κ_R . It would never reach the critical line where $\xi = \infty$, and accordingly there would not be a continuum quantum field theory with a fixed $\kappa_R > 0$.

quantum field theory can be expressed in terms of the bare coupling constants and the cut-off used to define the theory. Here we use a lattice regularization and the cut-off is the lattice spacing a , which we in (62) have put to 1. For all renormalized observables $\mathcal{O}_R(\kappa_0, a)$, the value should be independent of a when a is small (compared to any physical length scale in the theory). This will only be possible if we change κ_0 at the same time as we change a . Thus we have to write $\mathcal{O}_R(\kappa_0(a), a)$, where

$$0 = a \frac{d}{da} \mathcal{O}_R(\kappa_0(a), a) = \left(a \frac{\partial}{\partial a} + a \frac{d\kappa_0(a)}{da} \frac{\partial}{\partial \kappa_0} \right) \mathcal{O}_R(\kappa_0(a), a). \quad (63)$$

This is the simplest Callen-Symanzik equation. In particular we can apply it to $\kappa_R(\kappa_0(a), a)$. Finally, we can relate the cut-off a to the correlation length ξ by insisting that the physical correlation length $\ell_{phys} = \xi a$ stays fixed when $a \rightarrow 0$. This is equivalent to saying that the lattice exponential decay of the two-point function survives in the continuum when $a \rightarrow 0$, and that this exponential decay, which defines the renormalized mass m_R in the ϕ^4 theory, is given by

$$\frac{1}{\xi} = m_R a. \quad (64)$$

Introducing ξ instead of a in the Callen-Symanzik equation (63) we obtain

$$0 = \xi \frac{d}{d\xi} \kappa_R(\kappa_0(\xi), \xi) = \xi \frac{\partial \kappa_R}{\partial \xi} \Big|_{\kappa_0} + \frac{\partial \kappa_R}{\partial \kappa_0} \Big|_{\xi} \xi \frac{d\kappa_0}{d\xi} \Big|_{\kappa_R} \quad (65)$$

The curves $\kappa_R(\kappa_0(\xi), \xi) = \text{const.}$ are the ones shown in Fig. 8 for different choices of the value of κ_R . The renormalized value κ_R is fixed not at the UV fixed point κ_0^{uv} , but by the approach to it and the same is true for the other renormalized coupling constant, m_R . In this sense κ_R and m_R are free parameters in the renormalized theory.

Introducing the β -functions²⁰

$$\beta_0(\kappa_0) = \xi \frac{d\kappa_0}{d\xi} \Big|_{\kappa_R}, \quad \beta_R(\kappa_R) = -\xi \frac{\partial \kappa_R}{\partial \xi} \Big|_{\kappa_0}, \quad (66)$$

²⁰ Only when we are close to the critical line, i.e. when ξ is very large, will $\xi \partial \kappa_R(\kappa_0(\xi), \xi) / \partial \xi$ be a function only of κ_R . A similar statement is true for $\xi d\kappa_0 / d\xi$. We will assume we are in this so-called scaling region of coupling constant space. The reason for the different sign appearing in the two equations in (66) is that the change in κ_R is usually defined wrt a change of a physical mass scale like m_R in (64).

Eq. (65) can be written as

$$\beta_R(\kappa_R) = \frac{\partial \kappa_R}{\partial \kappa_0} \beta_0(\kappa_0) \quad (67)$$

and the two β -functions will have the same sign, but the sign difference in the definition (66) means that the behavior of $\kappa_0(\xi)$ and $\kappa_R(\xi)$ will be different when one solves Eq. (66) for $\xi \rightarrow \infty$, i.e. when approaching the critical line. The β -function $\beta_0(\kappa_0)$ in our ϕ^4 example is assumed to be zero at the fixed points and positive in the interval $\kappa_0^{\text{IR}}(1), \kappa_0^{\text{UV}}$ (and negative in the interval $\kappa_0^{\text{UV}}, \kappa_0^{\text{IR}}(2)$). Thus $\kappa_0 \rightarrow \kappa_0^{\text{UV}}$ when $\xi \rightarrow \infty$, (and by definition one follows a path where κ_R is kept fixed). On the other hand, solving (66) for κ_R we find that κ_R will be repelled by κ_0^{UV} and move towards one of the IR fixed points when $\xi \rightarrow \infty$, as one can see in Fig. 8. As a simple toy example to illustrate the behavior let us assume the β -function for the ϕ^4 is given by

$$\beta(\kappa) = \frac{c_0 \kappa^2 (\kappa^{\text{UV}} - \kappa)}{\nu c_0 \kappa^2 + (\kappa^{\text{UV}} - \kappa)}, \quad \beta_0(\kappa_0) = \beta(\kappa_0), \quad \beta_R(\kappa_R) = \beta(\kappa_R). \quad (68)$$

This toy β -function imitates the real ϕ^4 β -function to first order at the Gaussian IR fixed point $\kappa_0^{\text{IR}} = \kappa_R^{\text{IR}} = 0$ and has a UV fixed point at κ^{UV} . Also, it is a rational function of the coupling constant, a feature also present in the simplest FRG truncations.²¹ One can now solve for ξ and find

$$\xi(\kappa_0, \kappa_R) = \frac{f(\kappa_R)}{f(\kappa_0)}, \quad f(\kappa) = e^{1/c_0 \kappa} (\kappa^{\text{UV}} - \kappa)^\nu, \quad 0 < \kappa < \kappa^{\text{UV}}. \quad (69)$$

For fixed κ_R it will reproduce a sequence of curves like the ones shown at the left side of κ_0^{UV} in Fig. 8. Let us finally note that if the IR fixed point is characterized by an exponent ν_{IR} and the UV fixed point by an exponent ν_{UV} a toy model beta function will be

$$\beta(\kappa) = \frac{(\kappa - \kappa^{\text{IR}})(\kappa^{\text{UV}} - \kappa)}{\nu_{\text{IR}}(\kappa^{\text{UV}} - \kappa) + \nu_{\text{UV}}(\kappa - \kappa^{\text{IR}})}, \quad \beta_0(\kappa_0) = \beta(\kappa_0), \quad \beta_R(\kappa_R) = \beta(\kappa_R), \quad (70)$$

and one finds

$$\xi(\kappa_0, \kappa_R) = \frac{f(\kappa_R)}{f(\kappa_0)}, \quad f(\kappa) = \frac{(\kappa^{\text{UV}} - \kappa)^{\nu_{\text{UV}}}}{(\kappa - \kappa^{\text{IR}})^{\nu_{\text{IR}}}}, \quad \kappa^{\text{IR}} < \kappa < \kappa^{\text{UV}}. \quad (71)$$

It should be mentioned that the recently calculated β -function for $\lambda_k g_k$ in FRG has precisely the form (70), except that it is more complicated far away from κ^{IR} and κ^{UV} [12].

Let us also mention that irrespectively of the detailed form of the β -function, if we on the lattice observe a divergent correlation length ξ for $\kappa_0 \rightarrow \kappa_0^{\text{UV}}$ of the form

$$\xi \propto \frac{1}{(\kappa_0^{\text{UV}} - \kappa_0)^{\nu_{\text{UV}}}}, \quad \text{i.e.} \quad \kappa_0(\xi) = \kappa_0^{\text{UV}} - \frac{c}{\xi^{1/\nu_{\text{UV}}}} \quad (72)$$

then (66) leads to

$$\beta(\kappa_0) \approx \beta'(\kappa_0^{\text{UV}})(\kappa_0 - \kappa_0^{\text{UV}}) = -\frac{1}{\nu_{\text{UV}}}(\kappa_0 - \kappa_0^{\text{UV}}), \quad \text{i.e.} \quad \nu_{\text{UV}} = -\frac{1}{\beta'(\kappa_0^{\text{UV}})}. \quad (73)$$

To summarize: keeping the renormalized coupling κ_R fixed and taking the lattice correlation length to infinity, the lattice coupling constant κ_0 flows to the UV fixed point κ_0^{UV} , while keeping κ_0 fixed while taking the lattice correlation length to infinity results in a flow of the renormalized coupling constant to an IR fixed point κ_R^{IR} .

Application to CDT

We now want to apply this philosophy to the CDT lattice theory and we assume that the FRG effective action is expressed in terms of renormalized quantities. We have three dimensionless coupling constants, κ_4 , κ_0 and Δ . κ_4

²¹ In general $\beta_0(\kappa_0)$ and $\beta_R(\kappa_R)$ will not be identical, but one can show that the two first coefficients when expanding around a Gaussian fixed point are the same. Further, if the derivatives of the β -functions are different from zero at the UV fixed point (like here) they have to agree.

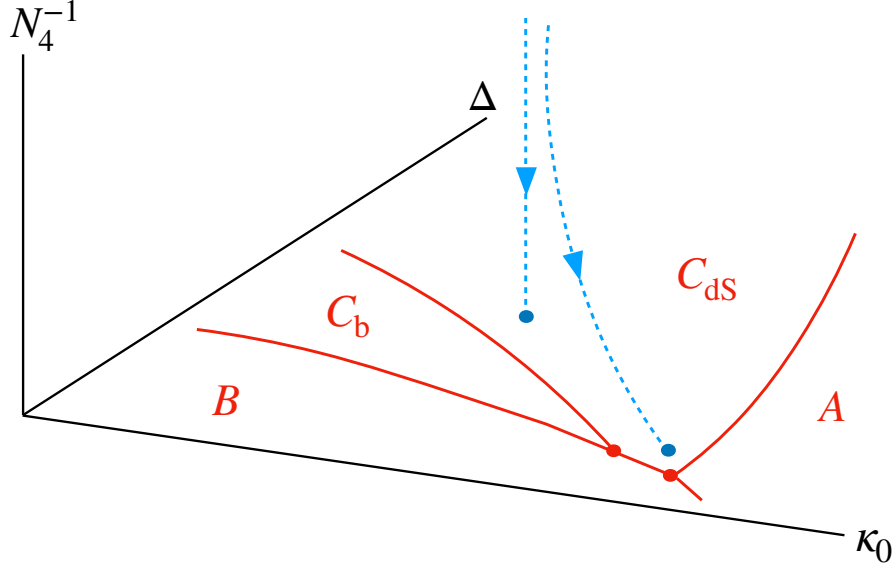


FIG. 9. The CDT phase diagram where N_4^{-1} is also included. Criticality can only occur when $N_4^{-1} = 0$. The straight vertical dashed line corresponds to keeping the bare lattice coupling constants κ_0, Δ fixed, while the other dashed line illustrates the flow when the renormalized coupling constants are fixed and one has to change the lattice coupling constants when approaching the critical surface.

is the coupling constant multiplying N_4 , the number of four-simplices, and as discussed in the main text there is a $\kappa_4^c(\kappa_0, \Delta)$ such that $\langle N_4 \rangle \rightarrow \infty$ for $\kappa_4 \rightarrow \kappa_4^c(\kappa_0, \Delta)$. We will be using N_4 as a variable instead of κ_4 , performing MC simulations for various values of N_4 . As discussed in the main text, the relevant correlation length related to the finite-size scaling observed in phase C_{dS} [14, 20], is the point-point correlation, a correlation unique for quantum gravity and for fixed (and large) N_4 it will be proportional to a typical linear size of a universe of spacetime volume N_4 , i.e. in the case of 4d CDT to $N_4^{1/4}$:

$$\xi \propto N_4^{1/4}. \quad (74)$$

The critical surface of the lattice theory will be for $N_4^{-1} \rightarrow 0$. The corresponding CDT phase diagram is shown in Fig. 9 as a function of κ_0, Δ and N_4^{-1} . For fixed bare coupling constants κ_0, Δ we thus expect that the renormalized coupling constants will flow towards their values at an IR fixed point. Similarly, we expect that for fixed renormalized values of the coupling constants we have to change κ_0 and Δ as functions of N_4 , when approaching the critical surface $N_4 = \infty$, in order to keep the renormalized coupling constants fixed. This is illustrated by the two curves shown in Fig. 9 that should be viewed as the equivalent to the ϕ^4 diagram shown in Fig. 8. Unfortunately we do not know how to calculate the renormalized coupling constants corresponding to the lattice theory, and as discussed in the main text we just assume that they can be identified with the renormalized coupling constants in the simplest possible FRG model. Thus for fixed lattice coupling constants κ_0, Δ the basic equation (23) tells us

$$\lambda_k g_k \propto \frac{\Gamma}{\xi^2}, \quad \text{i.e.} \quad \xi \frac{d}{d\xi} (\lambda_k g_k) = -2\lambda_k g_k. \quad (75)$$

This is indeed in agreement with (31) since near the Gaussian fixed point or the IR fixed point we also have from (23) that $\xi \propto k^{-2}$, more specifically (from (24) and (27)):

$$\xi \propto \frac{\sqrt{\Gamma}}{G_0 k^2} \quad (\text{Gaussian}), \quad \xi \propto \frac{\sqrt{\Gamma} k_0^2}{k^2} \quad (\text{IR}). \quad (76)$$

In the notation of (70) and (71) we have an IR fixed point with $\nu_{\text{IR}} = 2$.

Let us now discuss how to deal with the UV lattice fixed point. According to the discussion above we should now keep to renormalized coupling constant fixed, but it can be assigned any value between the IR value and the UV

value. Viewing $\lambda_k g_k$ for some value of k as one of these values, Eq. (23) implies (as already mentioned) that we should follow a path $(\kappa_0(N_4), \Delta(N_4))$ such that

$$\Gamma(\kappa_0(N_4), \Delta(N_4), N_4) \propto \sqrt{N_4} \quad (\propto \xi^2). \quad (77)$$

Let us for simplicity of the discussion ignore the coupling constant Δ , and likewise we will for the same reason ignore that the observed ω is not equal to ω_0 corresponding to a 4-sphere. This last point is discussed in detail in the main text. Finally let κ_0^{UV} denote the putative UV fixed point with exponent ν_{UV} . Assume that $\Gamma(\kappa_0)$ has the following behavior on the critical surface $N_4 = \infty$, close to κ_0^{UV} :

$$\Gamma(\kappa_0, N_4 = \infty) \propto \frac{1}{(\kappa_0^{\text{UV}} - \kappa_0)^\alpha} \quad (78)$$

Strictly speaking for a finite N_4 we do not have a critical point κ_0^{UV} , but only a so-called pseudo-critical point $\kappa_0^{\text{UV}}(N_4) < \kappa_0^{\text{UV}}$ and we expect

$$\kappa_0^{\text{UV}}(N_4) = \kappa_0^{\text{UV}} - \frac{c}{N_4^{1/4\nu_{\text{UV}}}}, \quad \xi \propto N_4^{1/4} \propto \frac{1}{(\kappa_0^{\text{UV}} - \kappa_0(N_4))^{\nu_{\text{UV}}}}. \quad (79)$$

It is thus natural to identify the exponent ν_{UV} introduced this way with the exponent ν_{UV} we encountered in our ϕ^4 discussion. Since for a given N_4 we cannot really choose $\kappa_0 > \kappa_0^{\text{UV}}(N_4)$ there is one “natural” way to approach the UV fixed point κ_0^{UV} corresponding to $N_4 = \infty$, namely to follow the path $\kappa_0^{\text{UV}}(N_4)$. In this case we obtain

$$\Gamma(\kappa_0^{\text{UV}}(N_4), N_4) \propto \frac{1}{(\kappa_0^{\text{UV}} - \kappa_0^{\text{UV}}(N_4))^\alpha} \propto N_4^{\alpha/4\nu_{\text{UV}}}. \quad (80)$$

This will be an upper bound on $\Gamma(\kappa_0(N_4), N_4)$ since $\kappa_0(N_4)$ is less than the pseudo-critical $\kappa_0^{\text{UV}}(N_4)$. Comparing this to (77) we have to have

$$\frac{\alpha}{4\nu_{\text{UV}}} \geq \frac{1}{2}, \quad (81)$$

and in order to approach the UV fixed point κ_0^{UV} such that (77) is satisfied one should choose a path

$$\kappa_0(N_4) = \kappa_0^{\text{UV}} - \frac{c}{N_4^{1/2\alpha}}. \quad (82)$$

Eq. (81) implies that we indeed have $\kappa_0(N_4) \leq \kappa_0^{\text{UV}}(N_4)$. The situation is illustrated in Fig. 10.

Assuming $\xi \propto N_4^{1/4}$ and using (73) makes it tempting to conjecture that the β -function for κ_0 will satisfy

$$\theta_{\kappa_0^{\text{UV}}} \equiv \beta'(\kappa_0^{\text{UV}}) = -\frac{2}{\alpha} \quad (83)$$

We will use this in the main article, but it should be kept in mind that the behavior (82) was obtained by assuming that the renormalized coupling ΛG was kept fixed, not the renormalized version of the lattice coupling κ_0 , which we strictly speaking do not know. However, since $\theta_{\kappa_0^{\text{UV}}} = \theta_{f(\kappa_0^{\text{UV}})}$ for any reasonable function $f(\kappa_0)$ where $f'(\kappa_0^{\text{UV}}) \neq 0$, the critical exponent $\theta_{\kappa_0^{\text{UV}}}$ might be the correct critical exponent for the bare lattice version of ΛG .

Remarks about first order transitions

The discussion above assumes a divergent correlation length at the phase transition point or line. First order transitions do usually not have such a divergent correlation length, which is one of the reasons one cannot use it to define a continuum field theory, starting from a lattice field theory. However, in the case of quantum gravity the situation can be different, the reason being that the divergent correlation length we have been discussing, coming from the point-point correlation function, the continuum version of which is defined by Eq. (61), is not necessarily related to the order parameter that defines the first order transition. In such a case, we might observe a double peak in the probability distribution of the order parameter that classifies the transition as first order. We have such a situation in the case of the $A - C_{\text{dS}}$ transition. The maxima of these peaks for a finite N_4 will be located at $\kappa_0^{(1)}(N_4) < \kappa_0^{(2)}(N_4)$, and they do not merge for $N_4 \rightarrow \infty$. Coming from phase C_{dS} we will first meet $\kappa_0^{(1)}(N_4)$ and this line will then serve

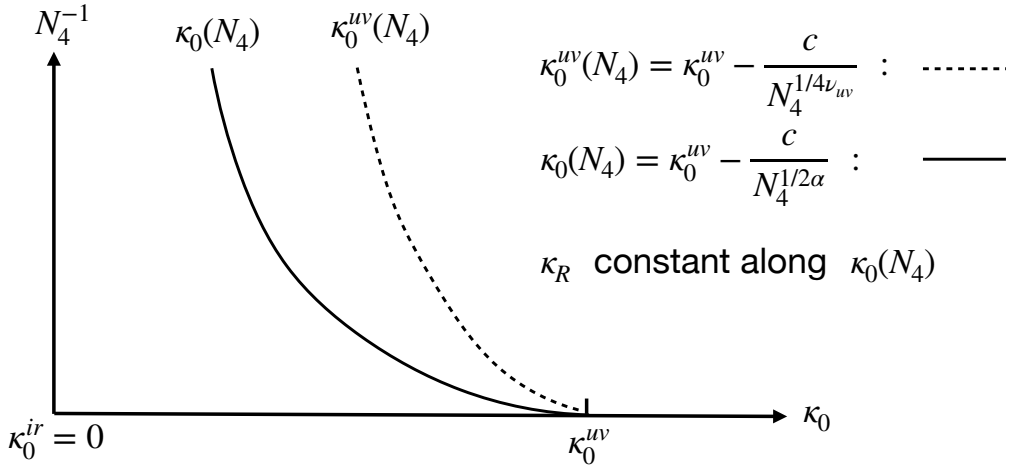


FIG. 10. The tentative CDT phase diagram (κ_0, N_4^{-1}) (with coupling constant Δ ignored). Pseudo-criticality appears along the dotted line $\kappa_0^{\text{UV}}(N_4)$ and the line $\kappa_0(N_4)$, where κ_R is constant is shown to the left of $\kappa_0^{\text{UV}}(N_4)$, $\kappa_R \propto \lambda_k g_k$. The critical line is $N_4^{-1} = 0$.

as the pseudo-critical line discussed above, and the correlation length $\xi = N_4^{1/4}$ related to the two-point function can still diverge for $N_4 \rightarrow \infty$ in the way discussed above. This is the scenario that we have in mind related to the A – C_{dS} transition.

We can of course force the system to cross the pseudo-critical line $\kappa_0^{(1)}(N_4)$ and move towards the other pseudo-critical line $\kappa_0^{(2)}(N_4)$ that would be met from phase A . During such a forced motion the geometries would be mixtures of phase C_{dS} and phase A geometries, and one would not have the phase C_{dS} effective action with the finite-size scaling that we have used and that we have related to the FRG action.

[1] J. Ambjorn, A. Goerlich, J. Jurkiewicz, and R. Loll, Nonperturbative Quantum Gravity, *Phys. Rept.* **519**, 127 (2012), arXiv:1203.3591 [hep-th].

[2] R. Loll, Quantum Gravity from Causal Dynamical Triangulations: A Review, *Class. Quant. Grav.* **37**, 013002 (2020), arXiv:1905.08669 [hep-th].

[3] S. Weinberg, *General Relativity: An Einstein Centenary Survey* (1980) pp. 790–831.

[4] A. Codello, R. Percacci, and C. Rahmede, Investigating the ultraviolet properties of gravity with a wilsonian renormalization group equation, *Annals of Physics* **324**, 414 (2009).

[5] M. Reuter and F. Saueressig, Quantum einstein gravity, *New Journal of Physics* **14**, 055022 (2012).

[6] M. Reuter and F. Saueressig, *Quantum Gravity and the Functional Renormalization Group: The Road towards Asymptotic Safety*, Cambridge Monographs on Mathematical Physics (Cambridge University Press, 2019).

[7] K. S. Stelle, Renormalization of higher-derivative quantum gravity, *Phys. Rev. D* **16**, 953 (1977).

[8] J. Ambjorn, J. Jurkiewicz, and R. Loll, Dynamically triangulating Lorentzian quantum gravity, *Nucl. Phys. B* **610**, 347 (2001), arXiv:hep-th/0105267.

[9] R. Ferrero and M. Reuter, Towards a geometrization of renormalization group histories in asymptotic safety, *Universe* **7**, 10.3390/universe7050125 (2021).

[10] R. Ferrero and M. Reuter, The spectral geometry of de sitter space in asymptotic safety, *J. High Energ. Phys.* (2022).

[11] B. Knorr and F. Saueressig, Towards reconstructing the quantum effective action of gravity, *Phys. Rev. Lett.* **121**, 161304 (2018).

[12] H. Kawai and N. Ohta, Wave function renormalization and flow of couplings in asymptotically safe quantum gravity, *Phys. Rev. D* **107**, 126025 (2023), arXiv:2305.10591 [hep-th].

[13] A. Baldazzi and K. Falls, Essential Quantum Einstein Gravity, *Universe* **07**, 294 (2021), arXiv:2107.00671 [hep-th].

[14] J. Ambjorn, A. Gorlich, J. Jurkiewicz, and R. Loll, The Nonperturbative Quantum de Sitter Universe, *Phys. Rev. D* **78**,

063544 (2008), arXiv:0807.4481 [hep-th].

[15] I. Montvay and G. Munster, Quantum fields on a lattice, Cambridge Monographs on Mathematical Physics (Cambridge University Press, 1997).

[16] J. Ambjorn and Y. Watabiki, Scaling in quantum gravity, *Nucl. Phys. B* **445**, 129 (1995), arXiv:hep-th/9501049.

[17] J. Ambjørn, B. Durhuus, and T. Jonsson, Quantum Geometry: A Statistical Field Theory Approach, Cambridge Monographs on Mathematical Physics (Cambridge Univ. Press, Cambridge, UK, 2005).

[18] J. Ambjorn and R. Loll, Nonperturbative Lorentzian quantum gravity, causality and topology change, *Nucl. Phys. B* **536**, 407 (1998), arXiv:hep-th/9805108.

[19] J. Ambjorn, J. Jurkiewicz, and R. Loll, Reconstructing the universe, *Phys. Rev. D* **72**, 064014 (2005), arXiv:hep-th/0505154.

[20] J. Ambjorn, S. Jordan, J. Jurkiewicz, and R. Loll, Second- and First-Order Phase Transitions in CDT, *Phys. Rev. D* **85**, 124044 (2012), arXiv:1205.1229 [hep-th].

[21] J. Ambjorn, J. Gizbert-Studnicki, A. Görlich, J. Jurkiewicz, and R. Loll, Renormalization in quantum theories of geometry, *Front. in Phys.* **8**, 247 (2020), arXiv:2002.01693 [hep-th].

[22] J. Ambjorn, A. Görlich, J. Jurkiewicz, A. Kreienbuehl, and R. Loll, Renormalization Group Flow in CDT, *Class. Quant. Grav.* **31**, 165003 (2014), arXiv:1405.4585 [hep-th].

[23] N. Christiansen, B. Knorr, J. M. Pawłowski, and A. Rodigast, Global Flows in Quantum Gravity, *Phys. Rev. D* **93**, 044036 (2016), arXiv:1403.1232 [hep-th].

[24] F. Saueressig and J. Wang, Foliated asymptotically safe gravity in the fluctuation approach, *JHEP* **09**, 064, arXiv:2306.10408 [hep-th].

[25] J. Ambjørn, D. Coumbe, J. Gizbert-Studnicki, A. Görlich, and J. Jurkiewicz, Critical Phenomena in Causal Dynamical Triangulations, *Class. Quant. Grav.* **36**, 224001 (2019), arXiv:1904.05755 [hep-th].

[26] P. Hořava, Quantum gravity at a lifshitz point, *Phys. Rev. D* **79**, 084008 (2009).

[27] D. N. Coumbe, J. Gizbert-Studnicki, and J. Jurkiewicz, Exploring the new phase transition of CDT, *JHEP* **02**, 144, arXiv:1510.08672 [hep-th].

[28] J. Ambjorn, D. Coumbe, J. Gizbert-Studnicki, A. Görlich, and J. Jurkiewicz, New higher-order transition in causal dynamical triangulations, *Phys. Rev. D* **95**, 124029 (2017).

[29] K. Falls and R. Ferrero, To appear, , (), : [].

[30] J. Ambjørn, A. Görlich, J. Jurkiewicz, R. Loll, J. Gizbert-Studnicki, and T. Trześniewski, The semiclassical limit of causal dynamical triangulations, *Nuclear Physics B* **849**, 144 (2011).

[31] J. Gizbert-Studnicki, Semiclassical and continuum limits of four-dimensional cdt, in Handbook of Quantum Gravity, edited by C. Bambi, L. Modesto, and I. Shapiro (Springer Nature Singapore, Singapore, 2023) pp. 1–43.

[32] J. Ambjorn, A. T. Goerlich, J. Jurkiewicz, and H. G. Zhang, Pseudo-topological transitions in 2D gravity models coupled to massless scalar fields, *Nucl. Phys. B* **863**, 421 (2012), arXiv:1201.1590 [gr-qc].

[33] J. Ambjørn, Z. Drogosz, J. Gizbert-Studnicki, A. Görlich, J. Jurkiewicz, and D. Németh, Matter-Driven Change of Space-time Topology, *Phys. Rev. Lett.* **127**, 161301 (2021), arXiv:2103.00198 [hep-th].

[34] J. Ambjorn and J. Jurkiewicz, Four-dimensional simplicial quantum gravity, *Phys. Lett. B* **278**, 42 (1992).

[35] J. Ambjorn and J. Jurkiewicz, Scaling in four-dimensional quantum gravity, *Nucl. Phys. B* **451**, 643 (1995), arXiv:hep-th/9503006.

[36] S. Bassler, J. Laiho, M. Schiffer, and J. Unmuth-Yockey, The de Sitter Instanton from Euclidean Dynamical Triangulations, *Phys. Rev. D* **103**, 114504 (2021), arXiv:2103.06973 [hep-lat].

[37] J. Laiho, S. Bassler, D. Coumbe, D. Du, and J. T. Neelakanta, Lattice Quantum Gravity and Asymptotic Safety, *Phys. Rev. D* **96**, 064015 (2017), arXiv:1604.02745 [hep-th].

[38] M. Lüscher and P. Weisz, Scaling Laws and Triviality Bounds in the Lattice ϕ^{*4} Theory. 1. One Component Model in the Symmetric Phase, *Nucl. Phys. B* **290**, 25 (1987).